Schweizerische Eidgenossenschaft
Confédération suisse
Confederazione Svizzera
Confederaziun svizra

Département fédéral de l'environnement,
des transports, de l'énergie et de la communication DETEC

Office fédéral de l'énergie OFEN

Project OFEN/BFE No 500,073

Geothermal Reservoir of the EGS Pilot Plant at Soultz-sous-Forêts (France): Monitoring of the Exploitation and Prediction of its Behaviour

Final Report, November 2012

Elaborated by the following member of DHMA:

Niels Giroud, François-David Vuataz, and Eva Schill,
Centre for Hydrogeology and Geothermics (CHYN)
University of Neuchâtel

Deep Heat Mining Association
c/o Häring Geo-Project
Im untern Tollacher
CH-8162 Steinmaur

Impressum

Date : Novembre 2012

Sur mandat de l’Office fédéral de l’énergie, contrat No 500’073-01 / projet No 500’073

Mühlestrasse 4, CH - 3063 Ittigen

Adresse postale : CH - 3003 Berne

www.bfe.admin.ch

Source d’acquisition de cette publication : www.recherche-energetique.ch

Table of Contents

Abstract

In the frame of the third research phase of the European Enhanced Geothermal System (EGS) project of Soultz-sous-Forêts (Alsace, France), the focus has been set on the behaviour of the geothermal reservoir upon long-term exploitation. Two 5,000 m deep and one 3,600 m deep wells are currently used to produce 1.5 MW of net electric power by the power plant that started in 2008. The period covered by this report ranges from 2009 to 2012, and has seen the longest fluid circulation period ever carried out at Soultz (323 days), which was an excellent opportunity to study the system's behaviour.

The Centre for Hydrogeology and Geothermics of the University of Neuchâtel focussed on the response of the geothermal reservoir to exploitation and chemical stimulation regarding water-rock interactions and their influence on the permeability and the productivity of the reservoir, using coupled thermal hydraulic and chemical (THC) numerical models. The report also analyses the evolution of the fluid composition with time and proposes some guidelines for the geochemical management of the complete geothermal loop in view of a durable exploitation of the reservoir for several decades.

Since the first production tests from the deep reservoir in 1999, the change of chemical composition of the fluid has been very limited, and the concentrations of dissolved components are only getting slightly closer to what is considered the Native Geothermal Brine (Sanjuan, 2010). The percentage of the total fluid originating from the massive volumes of cold and dilute water injected during boring as well as several stimulation events does probably not exceed 2 to 3 %. The single important modification of the total fluid composition that has been observed is the significant increase of the gas to liquid ratio, when sampled at the wellhead using a micro Webre separator, and which is mainly a consequence of an augmentation of the free CO_2 content of the fluid. One possible explanation of this phenomenon is calcite precipitation in the aquifer in the vicinity of the producing well (GPK2).

Numerical simulations were performed using the code FRAChem, a coupled THC code developed specifically at Neuchâtel for the Soultz project, in order to assess and understand the efficiency of the chemical stimulation operations performed on well GPK4 in 2006. The real-world stimulation improved the injectivity index by 35 %, and the computer model shows which minerals play a significant role in the stimulation process and also indicates a porosity increase from 10 % up to 17 % close to the wellbore, with an affected zone extending to 40 m from the well.

An executable version of the code FRAChem is provided with the report in order to allow the reader to perform circulation simulations of the fluid at Soultz in various conditions. Additionally, some simulations have been performed using the program TOUGHREACT, and show an increase of permeability close to the injection wells due to mineral dissolutions. According to the model, the injection in two different parts of the reservoir with different temperatures does not seem to affect significantly the permeability evolution of the reservoir. All in all, the simulated performance of the reservoir is very stable with time and no dramatic permeability loss can be foreseen with the computer models used in this study.

In order to maximise the durability of the Soultz-sous-Forêts EGS system, it is of greatest importance to monitor the fluid properties and try minimizing the potential of corrosion and scaling in the well and surface installations, and mineral precipitates affecting the reservoir permeability. During long-term exploitation, physical parameters of the fluid like temperature, pressure, flow-rate and electrical conductivity should be monitored at least on a weekly basis, both on the production and the injection lines, while major dissolved components can be measured in fluid samples once every three months. A complete set of analysis following careful sampling of both fluid phases is recommended once or twice a year. An unusual modification of any of the above mentioned parameters should give way to an immediate repetition of the measurement and, in case of one of the minor monitoring processes, to a complete sampling and analysis procedure in order to understand the potential causes of modification in the fluid composition.

1 Introduction

This report presents the results of the third research phase on the Soultz-sous-Forêts Enhanced Geothermal System (EGS) obtained by the Centre of Hydrogeology and Geothermics of the University of Neuchâtel. The European EGS project is located at Soultz-sous-Forêts in Alsace, France, about 50 km north of the city of Strasbourg (Figure 1). The project started in 1987 with the aim of producing electric power by using forced fluid circulation in a deep fractured crystalline rock. Three deep wells have been drilled to 5 km where the rock temperature reaches 200 °C. Many years of research helped to understand the geothermal reservoir, located in fractured granite within the Tertiary Rhine graben. The stimulation of the fractures partially clogged by naturally occurring hydrothermal minerals has improved the permeability of the reservoir and was followed by the construction of a pilot power plant in 2007–2008, which could be started in June 2008.

The two first phases of the research activities of the Swiss EGS R&D team under co-ordination of DHMA enhanced geothermal system spanned from 2001 to 2004 (André et al., 2005) and from 2004 to 2009 (Portier et al., 2009), respectively. The main focus of the Centre for Hydrogeology and Geothermics of the University of Neuchâtel during these two research phases consisted of the development and use of numerical simulation tools for predicting physical and chemical processes in the underground part of the geothermal system.

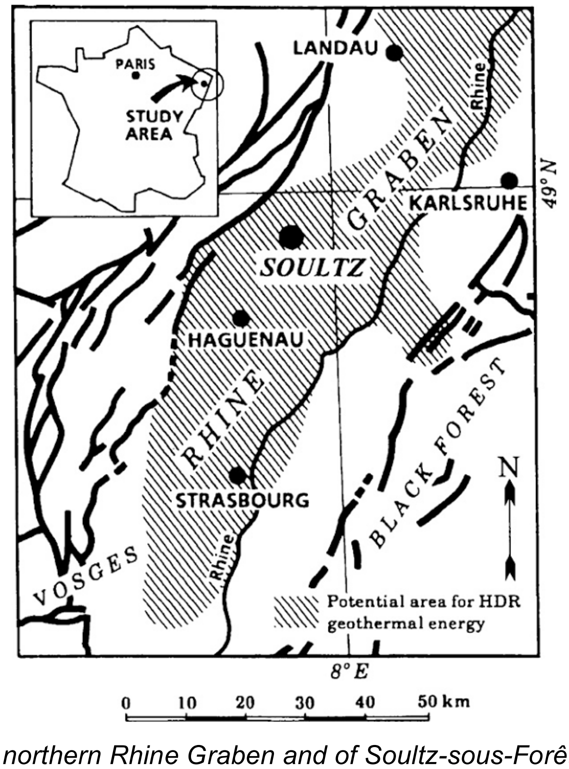

Figure 1: Location of the northern Rhine Graben and of Soultz-sous-Forêts (Sanjuan, 2010).

1.1 Objectives of this study

The current research phase started after the binary power plant was put into operation in 2008, and has therefore as major focus point the performance of the reservoir in the conditions of fluid circulation for electrical power production. The main objectives of the project for the University of Neuchâtel are to assess, by the means of numerical simulation, the geochemistry of the deep reservoir, the potential scaling and corrosion, and the effect of chemical stimulation. The initial contract covered a research period of three calendar years, between 2009 and 2011. However, the start of the third research phase for the French and German partners in the research program at Soultz was delayed until 2010. In order to increase the available geochemical and hydrological data for the simulations, the current project was stretched in order to cover the whole research program of our partners, despite its earlier start.

The numerical simulations were performed using the coupled thermal hydraulic chemical codes FRAChem and TOUGHREACT. The first one was specifically developed for the saline fluids and the geological settings of the EGS reservoir at Soultz and the latter is a commercial code developed at Lawrence Berkeley National Laboratory, USA, in a prototype version modified to implement the Pitzer formalism used in high ionic strength fluids for the calculation of ion activity coefficients.

This final reports presents the results of the implementation of chemical stimulations in the code FRAChem, the subsequent modifications made to that code, and an executable version of FRAChem with a complete description of the input and output files needed to simulate the circulation loop at the Soultz. With this executable and instructions, the user should be able to run numerical simulations of water rock interactions in the reservoir and to estimate the effect on the permeability of the reservoir rock. In addition, this report describes the result of numerical simulations of the latest circulation conditions, taking into account the changes in the geometry of the circulation loop for the long-term simulation runs.

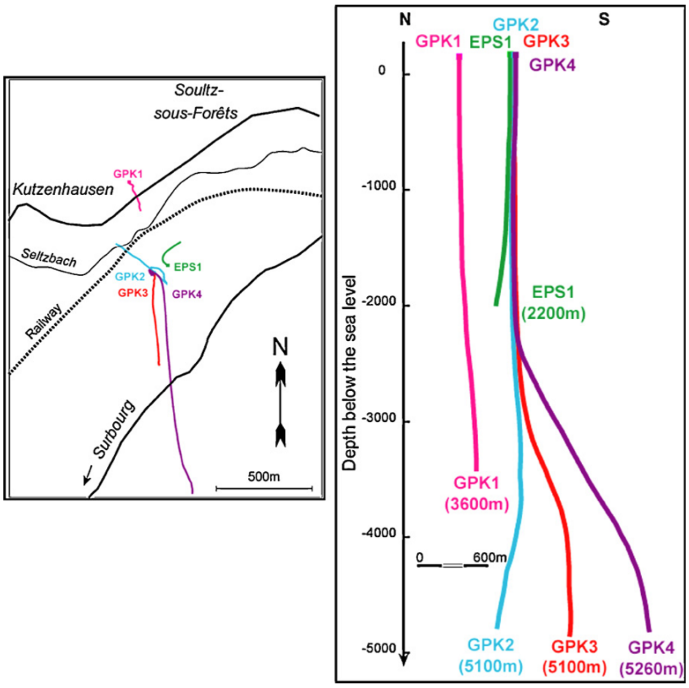

Figure 2: Map and profile showing the location of the four GPK wells. The EPS1 is an exploration well. (Dezayes, 2005)

1.2 On-site activity during this report period

During the four years covered by this report, several circulation tests have been performed at the Soultz site, using two to four of the wells. The complete circulation loop started operating as initially planned—production from wells GPK2 and GPK4 and reinjection in GPK3 (Figure 2)—but was subsequently modified due to the failure of the pump in well GPK4. In 2009, both the line shaft pump (LSP) in GPK2 and the electro submersible pump in GPK4 were used to produce geothermal fluid. The LSP pump in GPK2 operated between March and May and in October, while the ESP pump in GPK4 produced geothermal fluid from May until October, when it was permanently damaged. Between March and September, the fluid was mostly reinjected in GPK3, and in May and September–October reinjection also took place in GPK1.

After the failure of the ESP pump in GPK4, only one well (GPK2) is used for production and two are used for reinjection (GPK1 and GPK3). Between November 2009 and October 2010, the system was run for more than 320 days using this configuration, which was the longest non-stop circulation of the system since the beginning of the Soultz project. In October 2010, the loop was stopped to allow routine maintenance on the surface installations and on the LSP pump.

The circulation was started again in January 2011 using the same scheme, but with a higher production rate and with GPK1 replacing GPK3 as predominant injector, and continued until the end of the year, however with an interruption for maintenance between April and July. Figure 3 shows average flow rates and temperatures in the four wells during circulation tests from 2009 through 2011.

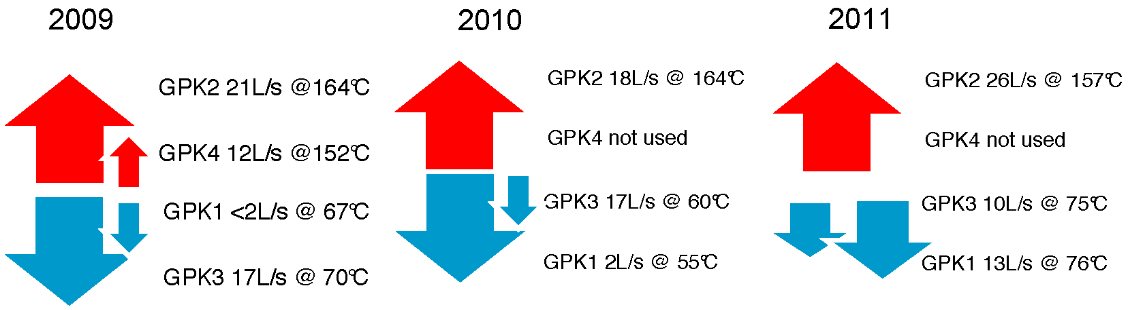

Figure 3: Schematic view of the circulation conditions between 2009 and 2011 with average flow-rates and fluid temperatures. Red arrows represent pumping from GPK2 and GPK4, and blue arrows represent reinjection in GPK1 and GPK3 (modified from Genter, 2011).

2 Simulation of chemical stimulation

In May 2006, well GPK4 was chemically stimulated in order to improve the permeability of the formation. To assess the chemical interactions between the host rock and a mixture of HCl and HF and their potential effects on the characteristics of the Soultz EGS reservoir, new modelling efforts using the FRAChem code have been initiated. This report presents the model calibration and results. The simulations consider realistic conditions with available data sets from the EGS system at Soultz. Results indicate that the predicted amount of fracture sealing minerals dissolved by the injection of an acidic solution (RMA) is consistent with the estimated amount of dissolved minerals during the chemical stimulation performed on well GPK4.

2.1 Addition of dissolution agents to FRAChem

2.1.1 Dissolving power of acids

The main readily HCl-soluble minerals are calcite, dolomite, and siderite, which additionally do not generate precipitates. The reactions are:

Calcite	$2HCl + CaCO_3 \rightarrow CaCl_2 + H_2O + CO_2$
Dolomite	$4HCl + CaMg(CO_3)_2 \rightarrow CaCl_2 + MgCl_2 + 2H_2O + 2CO_2$
Siderite	$2HCl + FeCO_3 \rightarrow FeCl_2 + H_2O + CO_2$

Siliceous minerals are dissolved by hydrofluoric acid and chemical reactions become significantly more complex with this acid as compared to HCl when carbonate minerals are involved (Walsh et al., 1982; Pournik, 2004). Quartz, clays, and feldspars are the main targets of sandstone acidizing. The chemical reactions are the following:

Quartz	$SiO_2 + 4HF \rightarrow SiF_4$ (silicon tetrafluoride) + $2H_2O$
	$SiF_4 + 2HF \rightarrow H_2SiF_6$ (fluosilicic acid)
Feldspars (Mg, Na or K)	$KAlSi_3O_8 + 14HF + 2H^+ \rightarrow K^+ + AlF_2 + 3SiF_4 + 8H_2O$
Clays:	
kaolinite	$Al_4Si_4O_{10}(OH)_8 + 24HF + 4H^+ \rightarrow 4AlF_2 + 4SiF_4 + 18H_2O$
montmorillonite	$Al_4Si_8O_{20}(OH)_4 + 40HF + 4H^+ \rightarrow 4AlF_2 + 8SiF_4 + 24H_2O$
illite	$K_{0.6}Mg_{0.25}Al_{2.3}Si_{3.5}O_{10}(OH)_2 + 18.6HF + 3.4H^+ \rightarrow 0.6K^+ + 0.25Mg^{++} + 2.3AlF_2 + 3.5SiF_4 + 12H_2O$

A convenient way to express the reaction stoichiometry is with the dissolving power of acids, introduced by Williams et al. (1979). The dissolving power expresses the amount of mineral that can be consumed by a given amount of acid on a mass or volume basis. X_g, the mass of mineral consumed by a given mass of acid, is defined as:

$$X_g = \frac{\nu_{mineral} M_{W,mineral}}{\nu_{acid} M_{w,acid}}$$

The dissolving power of any concentration of acid is the X_{g100} times the weight fraction of acid in the acid solution. For the commonly used preflush of 15 wt% HCl, $X_{g15}=0.15(X_{g100})$. The stoichiometric coefficients for common acidizing reactions are found from the reaction equations described above, while the molecular weights of the acids and minerals considered in the simulation are listed in Table 4 (Section 2.3 below).

The volumetric dissolving power, X_v, similarly defined as the volume of mineral dissolved by a given volume of acid, is related to the dissolving power X_g by:

$$X_v = X_g \frac{\rho_{acidsolution}}{\rho_{mineral}}$$

The volumetric dissolving power of HCl with calcite and dolomite and for HF with quartz and albite are given in Table 1.

Table 1: Volumetric dissolving power of RMA (acid mixture of 12%w/w HCl and 3%w/w HF)

Mineral	Volumetric dissolving power
Calcite	0.067
Dolomite	0.058
Quartz	0.010
K-feldspar	0.011

The volume of HCl preflush needed to consume the calcite within a short distance from the wellbore is the volume of calcite present divided by the volumetric dissolving power.

The main acid stage requires the greatest emphasis because of the damage mechanisms, directly associated to precipitation of products from the HF reactions (Allen and Roberts, 1989; Kalfayan, 2001). Acid stimulation techniques have to account for both chemistry and treatment execution to accurately predict the effectiveness since the effect of these precipitates could be minimized if they are deposited far from the wellbore (Entingh, 1999). A careful selection of mixtures, additives, acids formulations, and treatment volumes is the only way to minimize these secondary adverse effects.

2.1.2 Acid mineral reaction kinetics

Reaction rates are affected by kinetics; among the factors that strongly influence the mineral reactions are acid concentration and temperature. Dissolution reaction rates are proportional to the HF concentration for most sandstone minerals. The dissolution of minerals is a thermally activated phenomenon and the rates increase thus greatly as a function of temperature, while the penetration depth of live acid diminishes accordingly. Reaction kinetics data have been found in the literature for the reactions of HCl with calcite and dolomite and for the reactions of HF with quartz, feldspars and clays. Efforts have been made to develop FRAChem to simulate the acidizing process.

Acid-mineral reactions are termed heterogeneous reactions because they are reactions between species occurring at the interface between different phases, the aqueous acidic phase and the solid mineral. The reaction kinetics is a description of the rate at which the chemical reaction takes place, once the reacting species have been brought into contact.

The reaction rate for the HCl-$CaCO_3$ reaction is extremely high, so the overall rate of this reaction is usually controlled by the rate of acid transport to the mineral surface. On the other hand, the surface reaction rates for many HF-mineral reactions are very slow compared with the acid transport rate, and the overall rate of acid consumption or mineral dissolution is reaction rate controlled.

Reactions of HCl with carbonates

HCl is a strong acid, meaning that when HCl is dissolved in water, the acid molecules almost completely dissociate to form hydrogen ions, H^+, and chloride ions, Cl^-. The reaction between HCl and carbonate minerals is actually a reaction of the H^+ with the mineral. Lund et al. (1973, 1975) measured the kinetics of the HCl-calcite and HCl-dolomite reactions, respectively. Their results were summarized by Schechter (1992) as follows:

$$r_{carbonate} = sk_c \left(C_{HCl}\right)^{\alpha}$$

$$k_c = k_{c0} \exp\left(-\frac{E_a}{RT}\right)$$

where r is the reaction rate ($mol.s^{-1}$), C_{HCl} is HCl concentration ($mol.kg_{H2O}^{-1}$), k_c is the kinetic constant of the reaction ($mol.m^{-2}.s^{-1}$), s is the surface area of the mineral ($m^2.kg_{H2O}^{-1}$), E_a is the activation energy ($J.mol^{-1}$), R is the universal gas constant (8.3144 $J.mol^{-1}.K^{-1}$) and *T* is temperature (K). The constants are given in Table 6. SI units are used in these expressions.

Reaction of HF with sandstone minerals

HF reacts with virtually all of the many mineral constituents of sandstone. Reaction kinetics have been reported for the reactions of HF with quartz (Bergman, 1963; Hill et al., 1981), feldspars (Fogler et al., 1975), and clays (Kline and Fogler, 1981). These kinetics expressions can all be represented by:

$$r_{mineral} = sk_c\left[1 + K\left(C_{HCl}\right)^{\alpha}\right]\left(C_{HF}\right)^{\beta}$$

and the constants are given in Table 2.

These expressions show that the dependence on HF concentration is approximately first order (α = 1). For the feldspar reactions, the reaction rates increase with increasing HCl concentration, even though HCl is not consumed in the reaction. Therefore, HCl catalyses the HF-feldspar reactions. Also, the reaction rates between clay minerals and HF are very similar in magnitude, except for the illite reaction, which is about two orders of magnitude slower than the other reactions.

Table 2: Kinetic parameters used in the simulation

Mineral	α	β	***K***	$\boldsymbol{k_{c0}}$ ***(mol.m^{-2}.s^{-1})***	***Ea (kJ.mol^{-1})***
Calcite	0.63			7.314×10^{7}	62.8
Dolomite	$\frac{6.32\times10^{-4}T}{1-1.92\times10^{-3}T}$			4.48×10^{5}	65.7
Quartz	-	1	0	2.32×10^{-8}	9.56
K-feldspar	0.4	1.2	$5.66\times10^{-2}\,e^{(956/T)}$	1.27×10^{-1}	38.9
Albite	1	1	$6.24\times10^{-2}\,e^{(554/T)}$	9.5×10^{-3}	32.7
illite	-	1	0	2.75×10^{-2}	54.4

Per mass unit of rock, the specific surface area of each mineral is its specific surface area times the mass fraction of the mineral present in the sandstone. The fraction of HF expended in a particular reaction is the overall reaction rate for that mineral divided by the sum of the reaction rates. The reaction rates of HF with clays and feldspars are approximately two orders of magnitude higher than that between HF and quartz. Because of their relatively high reaction rates and low proportion in the total rock mass, clay minerals and feldspars will be consumed first in sandstone acidizing. The quartz reaction becomes predominant in regions where most of the clay and feldspar has already been dissolved.

2.2 Stimulation test on GPK4 in 2006

Hydrofluoric acid (HF) is the only common acid that dissolves clay, feldspar and quartz fines. For years mixtures of HF and HCl (RMA treatment) have been the standard acidizing treatment to dissolve these minerals that cause damage.

Regular Mud Acid (RMA) was injected from the wellhead through the casing string in GPK4 well. The stimulation zones were therefore the whole open hole section of the well (500 to 650 m length). In May 2006, the RMA treatment was carried out in four steps with addition of a corrosion inhibitor when needed. Before the injection of RMA, 2000 m^3 of cold deoxygenated water were introduced in the well at 12 L.s^{-1}, then at 22 L.s^{-1}, and finally at 28 L.s^{-1}. Later, to avoid calcium fluoride (CaF_2) precipitation that can lead to well damage, a preflush of 25 m^3 of a 15% solution of HCl in deoxygenated water (3.75 tons of HCl) was pumped ahead of the HCl-HF acid mixture for 15 minutes at 22 L.s^{-1}. A main flush consisting of a total of 200 m^3 of 12/3 (wt%) Regular Mud Acid (RMA) was then injected at a flow rate of 25 L.s^{-1} for 2.5 hours. Finally, a postflush of 2000 m^3 of cold deoxygenated water, at a flow rate of 22 L.s^{-1}, then 28 L.s^{-1} during 1 day, was injected after the RMA injection. The four stages are shown in Table 3.

Table 3: Four stages stimulation performed on GPK4 in May 2006

Fluid	**Volume (m^3)**	**Flow rate (l.s-^{1})**
Cold fresh water	2000	Successively 12, 22 and 28
Deoxygenated water with 15% HCl	25	22
RMA at 12/3 %	200	25
Cold deoxygenated water	2000	Successively 22 and 28

After the RMA stimulation, the wellhead pressure curve was smooth, indicating an efficient clean up of the hydrothermalised fracture or porous zones in the first ten meters surrounding the open hole (GEIE, 2006). The step rate test performed later in May 2006 (Figure 5), after the RMA-stimulation, shows that, after three days of injection, the wellhead pressure is about 65 bars, which is about 16 bars lower than before stimulation (step rate test performed on April 2006). This represents a 35 % reduction of the wellhead pressure due to acidification treatment (GEIE, 2006). Before the RMA treatment, the wellhead pressure curve raised with the flow increase showing a restricted storage capacity in the vicinity of the well. It can be estimated that the RMA-stimulation has therefore resulted in a maximum enhancement of the injectivity index of 35%. However, no production test was performed after these operations to verify the productivity index.

2.3 Description of the simulation

The mineral dissolution and porosity enhancement near the injection well following short acid mixture injection has been reproduced by simulation using FRAChem.

2.3.1 Geometrical and flow conditions

The present application of FRAChem is the modelling of a 2-D simplified model with a geometry close to the Soultz system. Injection and production wells are linked by fractured zones and surrounded by the impermeable granite matrix. The model is composed of 1250 fractured zones. Each fractured zone has an aperture of 0.1 m, a depth of 10 m, a porosity of 10%, and contains 200 fractures. This model allows an effective open thickness of about 125 m, while the mean open-hole section of each well is about 600 m. Initially the temperature was set to the reservoir temperature of 200°C and the fractured zone is filled with the initial formation fluid.

One of these fractured zones is modelled with the assumption that the fluid exchange with the surrounding low permeability matrix is insignificant. Due to the symmetrical shape of the model, only the upper part of the fractured zone is considered in the simulation. The area is discretized into 222 2D elements (Figure 4).

Considering the main flush injection rate of $22\,\mathrm{l\,s^{-1}}$, the fluid was re-injected in the modelled fractured zone at a rate of $1.76 \cdot 10^{-2}\,\mathrm{l\,s^{-1}}$. During this simulation, a constant overpressure of 70 bars was assumed at the injection well and an initial hydrostatic pressure of 500 bars was assumed for about 5000 m depth. The uncertainty on the permeability specification does not affect significantly the simulation results of reactive transport and porosity enhancement thanks to the constant injection rate. Dirichlet boundary conditions were applied to the upper, left and right side of the model. The values of thermo-hydraulic parameters considered in the simulation are listed in Table 4.

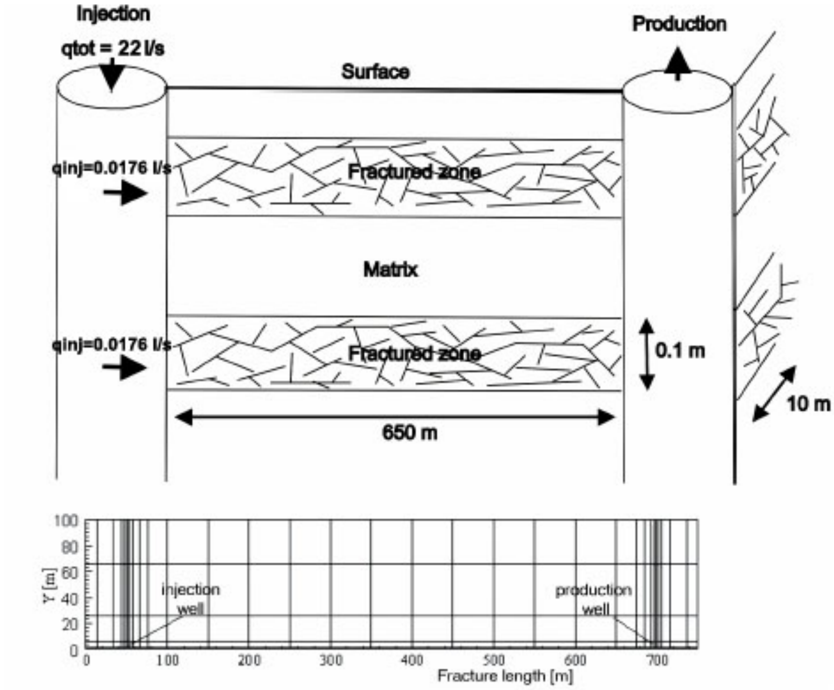

Figure 4: Simplified model and spatial discretization.

The injected fluid temperature was set to 65°C and its chemistry was the same as in the field test, i.e. 3 %w/w HF – 12 %w/w HCl solution, and a density of 1075 kg.m^{-3}. The initial reservoir fluid is in chemical equilibrium with the initial mineralogy at a reservoir temperature of 200°C. A maximum test-period of two days was simulated, including the injection of cold fresh water at 25°C, a preflush of 15 %w/w HCl solution during 0.25 hours and a postflush period of one day after the 2.5 hours of injection of RMA.

Table 4: Thermo-hydraulic parameters for the main flush

Reservoir properties			
Parameters	**Fracture**	**Matrix**	**Fluid**
Hydraulic conductivity [m^2.Pa^{-1}.s^{-1}]	7.4 10^{-8}	10^{-15}	-
Thermal conductivity [W.m^{-1}.K^{-1}]	2.9	3	0.6
Density [kg.m^{-3}]	-	2650	1000
Heat capacity [J.kg^{-1}.K^{-1}]	-	1000	4200
Porosity [%]	10	0	-
Initial and boundary conditions			
Initial reservoir temperature (°C)	200		
Injection overpressure (bar)	70		
Injection temperature (°C)	65		
Injection rate (L.s^{-1})	22		
Injection time (hours)	2.5		

2.3.2 Mineralogical and chemical settings

The mineralogical composition of the Soultz reservoir granite was described by Jacquot (2000) on the basis of data collected in well GPK2. It is assumed to be the same in all three wells (GPK2, GPK3 and GPK4) (Table 5). In the following simulation, the fluids are assumed to circulate within the hydrothermalised granite. Regarding the mineralogical composition of the fractured zone, only quartz (40.9 %), K-feldspar (13.9 %), albite (16.5 %), calcite (3.3 %), dolomite (0.8 %) and illite (24.6 %) are considered. The geothermal fluid present in the formation is a NaCl brine with a pH of 4.9, a total dissolved solids of about 100 g/l and a temperature at the beginning of the simulation of 200 °C. The main characteristics of this fluid are given in Table 6.

Table 5: Mean composition (in volume percent) of the different granite facies in the Soultz reservoir (Jacquot, 2000).

Minerals	**Healthy granite**	**Hydrothermalised granite**	**Alteration vein**
Quartz	24.2	40.9	43.9
K-Feldspar	23.6	13.9	
Plagioclases	42.5		
Illite		24.6	40.2
Smectite		9.7	9.6
Micas	9.3		
Calcite	0.3	3.3	4.3
Dolomite		0.8	0.7
Pyrite		0.7	1.0
Galena		1.3	0.3
Chlorite		4.8	

Table 6: Temperature (°C), pH, and concentrations of major species (mg kg^{-1}) of the formation brine used for the numerical simulation

Temperature	200
pH	4.9
Na^+	26400
K^+	2870
Ca^{2+}	6160
Mg^{2+}	112
Fe^{2+}	134
SiO_2	364
Cl^-	54205
SO_4^{2-}	63
HCO_3^-	58

Table 7: Molecular weight and density of the acids and minerals considered in the simulation

Compounds	Molecular weight (g mol^{-1})	Density (g cm^{-3})
HCl	63.5	15% HCl solution: 1.07
HF	20	3% HF-12% HCl solution: 1.075
Calcite	100.1	2.71
Dolomite	184.4	2.84
Siderite	115.8	3.94
Quartz	60.1	2.65
Albite	262.3	2.61
K-feldspars	278.4	2.5
Illite	389.3	2.75
Am.Silica	60.1	2.07

2.4 Simulation results

To validate the simulation described above, the numerical results were applied to hydraulic data measured during the RMA stimulation test. Since, in the numerical model, the pressure at the injection and the production point was fixed, pressure cannot be used for comparison. Instead, the evolution of transmissivity was compared between the model and the measured data.

Figure 5 shows the evolution of the pressure at GPK4 (injection well) during the stimulation test as well as the fluid injection rate.

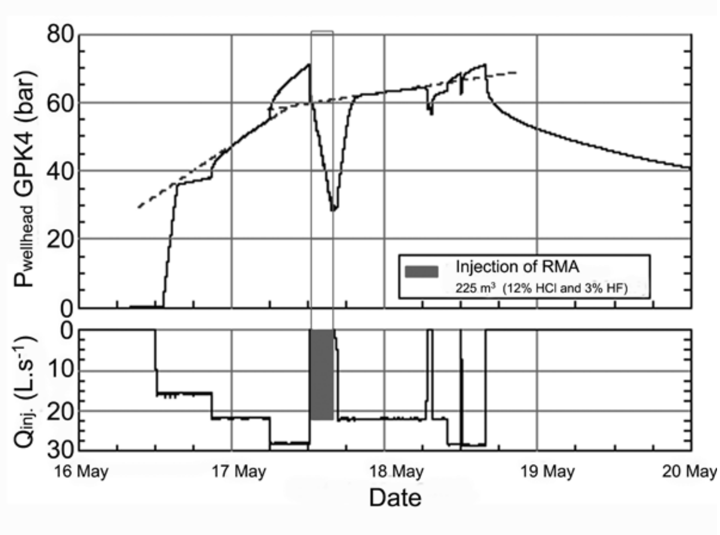

Figure 5: Impact of Regular Mud Acid acidification test performed on GPK4 in May 2006 (after Nami et al, 2007). The slope change of the pressure (dash line) for the same flow rate before and after RMA injection (preflush of 25 m^3 HCl at 15% and mainflush of 200 m^3.

The transmissivity, *T*, is calculated by:

$$T = \frac{q_{tot}}{L\left\|\nabla P\right\|}$$

q_{tot} is the fluid injection rate, L the depth of the fracture and ∇P the pressure gradient. In the case of the numerical model, L is 10 m, ∇P is constant, since the pressure was fixed at the injection and the production point. q_{tot} is calculated by:

$$q_{tot} = v_f A_i \Phi$$

v_f is the fluid velocity, A_i the area of the element interfaces and Φ the porosity. The resulting flow rate evolution in the fractured zone is illustrated in Figure 6.

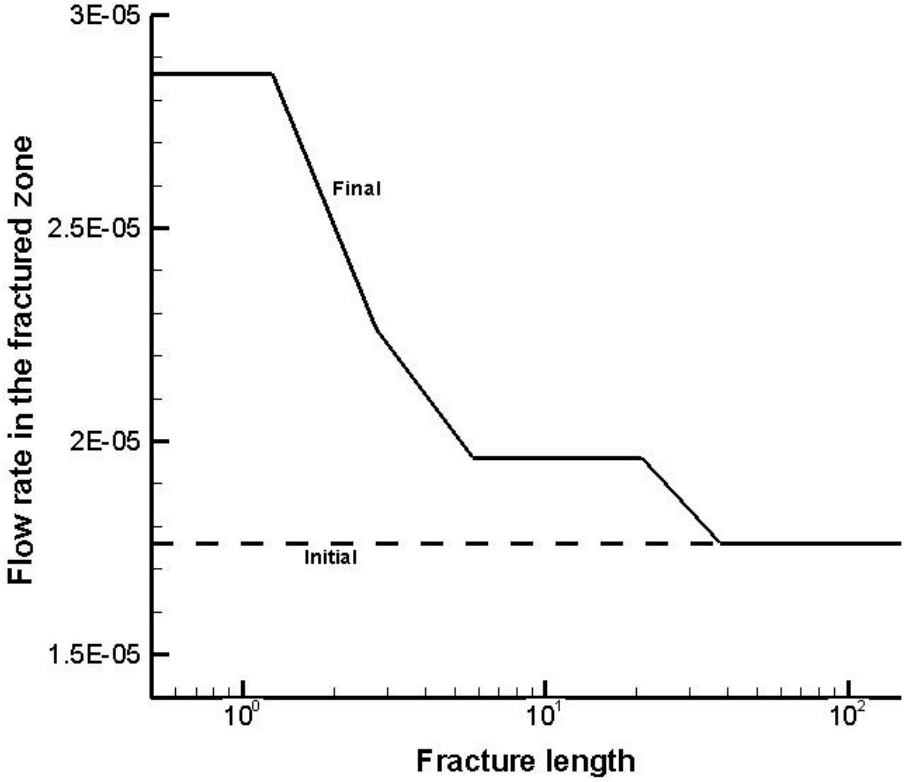

Figure 6: Resulting flow rate (in $m^3.s^{-1}$) evolution as a function of the fractured zone length (in m) from numerical model.

To calculate the transmissivity evolution during the stimulation test according to the numerical model, i.e. for a single fractured zone, the fluid injection rate is divided by the number of assumed fractured zones. ∇P is taken from the stimulation data. Due to different initial pressure conditions, the transmissivity in the numerical model is higher than that in the stimulation test. However, the transmissivity evolution as a percentage of the initial value in the first meters of the fractured zone increases in both cases by 35 %. The transmissivity increase in the stimulation test points to geochemical processes in the reservoir, such as the dissolution of calcite and feldspars. The good fit between the transmissivity evolution of the numerical model and the stimulation in the field confirms this assumption. The pressure evolution in the reservoir is therefore mainly the result of geochemical processes.

The overall enhancement of porosity and permeability obtained from the simulation is presented in Figure 7. The porosity increases to about 0.17 from an initial value of 0.10 close to the injection point. The enhancement of porosity extends to a distance of about

30 m. Increases in porosity are mainly caused by dissolution of calcite, K-Feldspar, albite and illite (Figure 8). Results show that acid preflush dissolves carbonates in the first metres of the fractured zone. Calcite dissolves with maximum amount of 3.3 % in the first 1.5 m from the injection point. The other minerals are not attacked by the 15 %w/w HCl solution. The injection of RMA leads to an increase of the size of the influenced zone, and at this stage, the first 40 m around the injection well are affected (Figure 8). Because the clay and feldspar reaction rates are relatively high and they form only a small portion of the total rock mass, they are consumed first in RMA acidizing. K-feldspar, illite and albite dissolution occurs close to the injection point (Figure 8). The quartz reaction becomes important in regions where most of illite and feldspars have already been dissolved. However, the amounts of quartz that are dissolved are very small because of the low reaction rate.

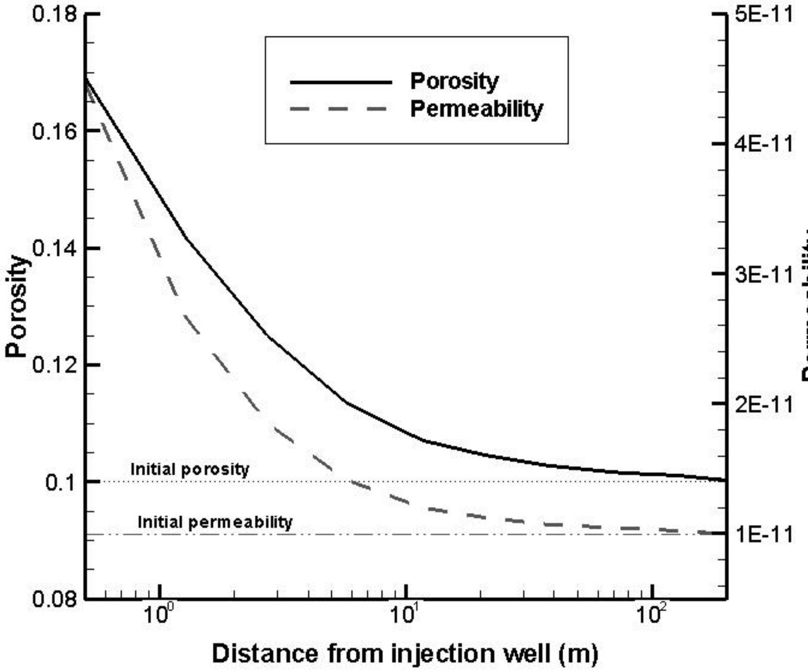

Figure 7: Distribution of porosity and permeability (in m^2) enhancement obtained from the simulation.

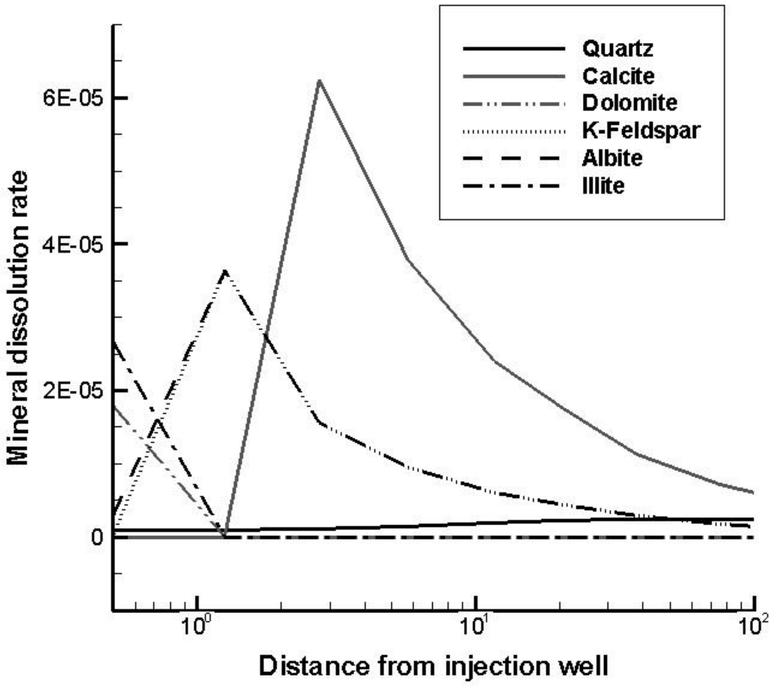

Figure 8: Evolution of the mineral dissolution rates (in mol.m^{-3}.s^{-1}) with distance (in m) following RMA injection.

3 Enhancement of the code FRAChem

An important part of this project for the University of Neuchâtel was dedicated to improving the code FRAChem for the numerical simulation of the circulation conditions in the Soultz reservoir. This section describes the main improvements brought to the software during this project time. The main modifications include the addition of the ability to simulate chemical stimulation processes in the reservoir (see section 1.2), the modification of the code for new hardware and software and other various small improvements in the chemistry part of the code.

An executable version of FRAChem is delivered on the CD-ROM attached to this report. The executable is specifically designed for the conditions encountered in the reservoir at Soultz regarding the rock and fluid composition and should allow the user to simulate the fluid circulation in the current loop and surface installations and to predict dissolution and precipitation processes in the aquifer. Appendix I delivers instructions on how to use the executable with a description of the input and output files.

3.1 Update for new hardware and software development tools

After the arrival of a new collaborator as the main developer working on the FRAChem project, replacing the collaborator who started the project, the main software used for developing the code (Microsoft Visual Studio ®) stopped working. This failure was most likely linked to so far unresolved permission problems for running the code on the same computer as before, but with a different user. These software obstacles were solved by the coinciding replacement of the hardware, according to the standard computer hardware replacement plan of the university.

However, the shift from Windows XP® to Windows 7® implied the installation of the latest version of the Visual Studio ® program and FORTRAN compiler. The latter two ended up being incompatible with some sections of the source code.

The main libraries, issued from the parent code for thermal and hydraulic coupling FRACTURE, needed to be modified and recompiled for the newer compiler version. This worked was performed in collaboration with GEOWATT AG.

3.2 Bug tracking and various improvements

To adapt the FRAChem source code to the new compiler required an important debugging process. Some unclear variable definitions, while accepted in the old compiler, were rejected in the new one. Each source code file has therefore been compiled in numerous small steps in the new compiler until the apparition of error messages in order to localize the source of the problem.

Figure 9 lists the source code files at the core of FRAChem. The file CHEMISTRY.F90 deals with the chemical reactions, while the other files, including the library are responsible with thermal and hydraulic processes and the coupling.

To correct the errors without introducing new ones requires controlling the declaration of the variables, at the beginning of the file or of a subroutine, and their subsequent use. Some of the subroutine declarations and their use in other subroutines has to be checked as well.

```
-  Chemistry.f90
-  DSLUBC.f90
-  Elast.f90
-  Element.f90
-  FRAChem_driver.f90
-  FRAChem4.f90
-  FraChemLib_Release.lib
-  Fract3a.f90
-  Module.f90
-  PD_Lapack.for
-  Thyd.f90
```

Figure 9: List of source code files of FRAChem.

Most modifications were brought on three files:

- FraChemLib_Release.lib : This library includes an important part of the code FRACTure that has already been compiled. This structure is highly time saving as it allows FRAChem to be compiled without the need to compile important sections of code that have not been modified. However, a compiled library is platform and compiler dependant, and the library had therefore to be modified in order to be used in the compilation of the updated FRAChem.
- A module hosted in the file Module.f90 had to be modified in order to allow FRAChem to be compiled on Intel Visual Studio. The dummy argument of a variable was set as a scalar instead of a vector, causing compilation error, although the older compiler did not report any error when compiling the same file.
- Most of the modifications and improvements of FRAChem are brought into the file Chemistry.f90, as it hosts the chemical reactions. In the hardware and software update process, we encountered some variable declaration problems that seemed to be overlooked by older compiling tools. The newer compiler was able to compile the Fortran code and produce an executable file, but the resulting executable would produce errors and abort.

Taking the opportunity to go through an important part of the chemical part of FRAChem, namely the file *Chemistry.f90*, the commenting was adjusted and extended, in order to improve the readability of the code and allow for faster modifications in the future.

On the other hand, care should be taken when the declaration of a variable that is used in many different subroutines is changed. In order to insure that no new errors were introduced by the modification, the use of the variable was tracked and analysed throughout the entire source code. Subsequently, we compared the output of two simulations performed with identical input files. One simulation was done with the executable file compiled on the latest compiler after the modification of the code, and the second simulation used an executable compiled on the Compaq Visual Fortran by the previous collaborator, i.e. without the code modification. Excepting from negligible rounding approximations, the comparison of the outputs showed that both simulations produced identical results, and we can therefore conclude that the modification was done in a way that no new error was introduced into the source code.

The stability of the calculations has been tested with many different simulation time frames, showing no more instabilities than previous versions. Calculation times are identical between the former and the newer versions of the code.

4 Simulation of modified circulation conditions at Soultz

The circulation concept of the EGS system at Soultz used the three deepest wells, all located on the same platform. However, in 2009, the ESP pump in well GPK4 broke down and the decision was made to continue the production from GPK2 only, without replacing the damaged pump, leaving well GPK4 unused. The circulation scheme used since 2009 include therefore pumping with the LSP pump in GPK2, and injecting in GPK3, but also in GPK1, which is located in the upper reservoir (Figure 10).

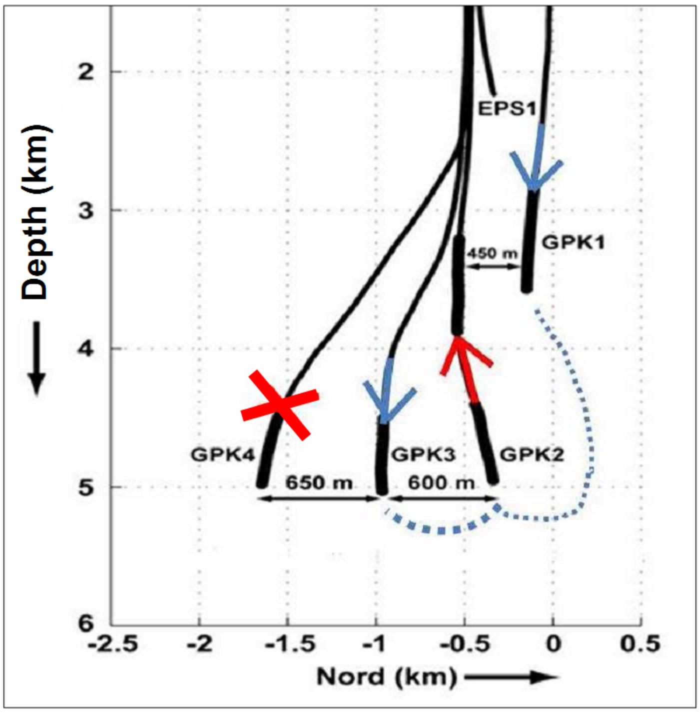

Figure 10: Schematic view of the circulation in 2010 and 2011 in the four deep wells at Soultz-sous-Forêts (Melchert, 2011)

4.1 Long-term circulation parameters

4.1.1 Physical parameters

Between November 2009 and October 2010, fluid was circulated continuously in the system for the longest period since the start of the EGS project at Soultz-sous-Forêts. The total circulation time reached 323 days. The fluid was produced from GPK2 at a rate of 18 l s^{-1} and reinjected in both GPK3 and GPK1. Most of the fluid was injected in well GPK3 at a rate of 15 to 17 l s^{-1}, while a testing flow rate of about 2 l s^{-1} was injected in GPK1 (Figure 11 and Table 8). The reinjection temperature was 60 °C in GPK3 and 55 °C in GPK1. During this circulation episode, the production temperature was about 164 °C.

In the numerical simulations performed previously on the deep reservoir, the injection rate was set to 20 l s^{-1} and an injection temperature of 65 °C was selected.

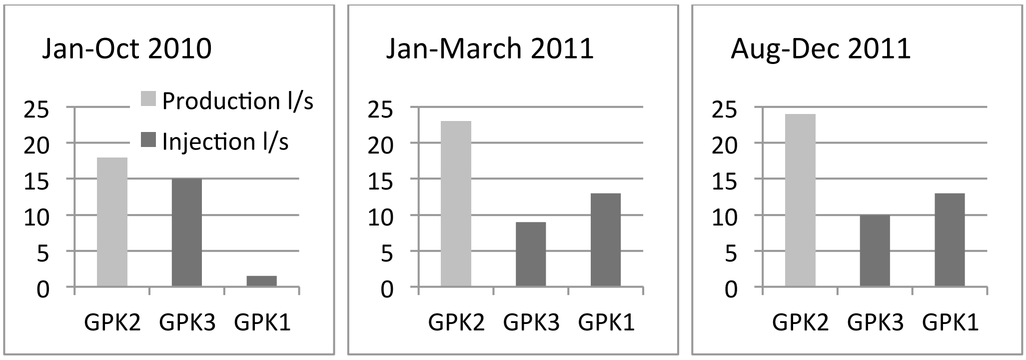

Figure 11: Injection and production rates during the fluid circulation in 2010 and 2011

At the beginning of 2011, after a shutdown period of two and a half months for maintenance, the production rate from GPK2 was increased to 23 l s^{-1}, from previously 18 l s^{-1} and at the same time the proportions between the injection rates in GPK3 and GPK1 were drastically modified (Figure 11). The flow rate injected in GPK1 was increased to 13 l s^{-1} while it was reduced to 9 l s^{-1} in GPK3. This flow rate increase in GPK1 led to a temperature decrease of ~5 °C of the produced fluid in GPK2 (159 °C).

After a careful monitoring of the reservoir response in terms of seismicity and temperature, the production rate from GPK2 was further increased to 24 l s^{-1} and the injection in GPK3 and GPK1 modified to 10 and 13 l s^{-1}, respectively.

Table 8: Thermo-hydraulic parameters of the 2009-2010 fluid circulation

Reservoir properties			
Parameters	Fracture	Matrix	Fluid
Hydraulic conductivity [$m^2.Pa^{-1}.s^{-1}$]	7.4 10^{-8}	10^{-15}	-
Thermal conductivity [$W.m^{-1}.K^{-1}$]	2.9	3	0.6
Density [$kg.m^{-3}$]	-	2650	1000
Heat capacity [$J.kg^{-1}.K^{-1}$]	-	1000	4200
Porosity [%]	10	0	-
Temperature (°C)		200	
Injection conditions			
Temperature (°C)		60	
Injection Overpressure (bar)		51	
Rate ($L.s^{-1}$)		17	

4.1.2 Chemistry

Previous simulations of fluid circulation in the Soultz-sous-Forêts geothermal reservoir were based on chemical analyses of samples taken at the wellhead of GPK2 in 1999 after 40 days of circulation. More than ten years of intermittent injection of cold fluid and a modification of the mineral paragenesis in the fractures in the vicinity of the wells may have impacted the chemistry of the fluid.

During the 320 days of fluid circulation in 2009–2010, fluid samples were collected at regular regularly and analyzed by the BRGM. The results of the analyses show only a small change in the chemical composition of the fluid between 1999 and 2010 (see section 5). In 2010, the fluid has lost a part of the injected fresh water component compared to samples from 2008, resulting in a slight increase in dissolved solids (Sanjuan, pers. comm.)

Gas samples collected by the BRGM show an important increase of the gas/liquid ratio in the total fluid discharged from GPK2 between 1999 and 2010, mostly due to an increase of the amount of CO_2. However, in 2010, the gas/liquid ratio is less than 0.2 %w/w in the discharged fluid. The increase of the mass of CO_2 in the gas phase is the consequence of a slight loss of CO_2 in the sampled water. This CO_2 loss is taken into account in the aquifer chemical composition calculation by assuming equilibrium with calcite. Considering the quality of the data of all the samples collected since 1999, the samples collected late 1999 seem to be the most representative of the original aquifer composition and are therefore used for the simulations.

4.2 *Simulations with TOUGHREACT*

4.2.1 Introduction

TOUGHREACT is a multiphase reactive transport simulator developed at Lawrence Berkeley National Laboratory (Xu and Pruess, 2001; Xu et al., 2004, Xu et al., 2006). The code is based on the finite difference code TOUGH2 (Pruess, 1991). TOUGHREACT is designed for a large variety of uses, from CO_2 sequestration to radioactive waste deposits and reactive flow in geothermal systems.

The base database for equilibrium constants comes mostly from SUPCRT92 (Johnson et al., 1992), and are given for temperatures between 0 and 300 °C and pressures of 1 bar up to 100 °C and vapour saturation pressure between 100 and 300 °C. Activities for dissolved gases are computed from data by Drummond (1981). The Pitzer ion-activity model was implemented in version 1.2 of TOUGHREACT (current version is 2.0), using the Harvie-Moller-Weare (HMW) formulation (Harvie et al., 1984) and ion-interaction parameters compiled and updated by Wolery et al. (2004). The EQ3/6 thermodynamic database data0.ypf (Wolery et al., 2004) was modified for $CO_{2(aq)}$ above 100 °C (André et al., 2006), using data from Rumpf et al (1994) and Rumpf and Maurer (1993).

Changes in porosity during the simulation are calculated from changes in mineral volume fractions. Several porosity-permeability and fracture aperture-permeability relationships are included in the model. Here, fracture porosity is related to permeability using the relationship proposed by Verma and Pruess (1988) and described in Xu et al. (2004). Mineral dissolution and precipitation can occur either by local equilibrium or by kinetic reaction. The kinetic model used here uses a general form of transition state theory rate law (Lasaga, 1984; Steefel and Lasaga, 1994; Palandri and Kharaka, 2004).

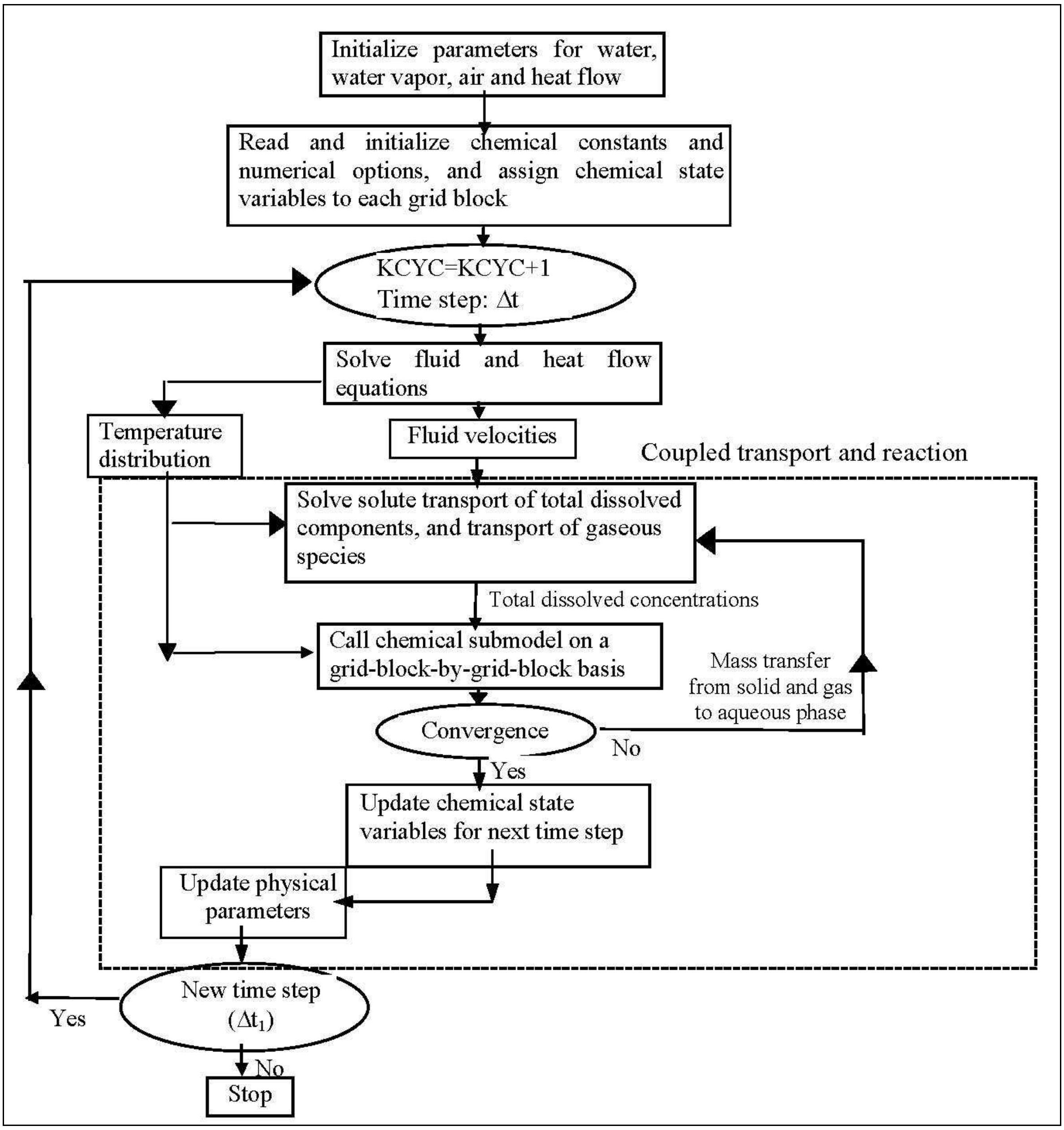

Figure 12: Flow chart of the TOUGHREACT code (Xu et al., 2004)

4.2.2 Model setup

The numerical model created for FRAChem includes matrix grid blocks, which have virtually no permeability and are used only for heat exchange with the fracture walls. In TOUGHREACT, heat loss is dealt with by a semi-analytical solution (Vinsome and Westerveld, 1980) built into the code. Therefore, the model is made of only 25 grid blocks representing the fracture between the injection and the production well. In our case, the coupling uses a sequential non-iterative approach (Figure 12).

For code stability reasons, the size of time-steps has been limited to 830 seconds. Total simulation times of 5 and 10 years have been selected for the forecast of permeability evolution of the fracture network upon forced fluid circulation.

The minerals computed in this model are the four most important phases observed in the altered granite rock of Soultz, namely quartz, K-feldspar, calcite and dolomite, as well as amorphous silica which is included in the model in order to be able to predict amorphous silica precipitation in the vicinity of the injection well.

As the volume of the reservoir (Aquilina, 2004, Sanjuan, pers.comm.) by far exceeds the volume of circulated fluid, and since the composition of the produced geothermal fluid has been relatively stable during more than ten years of various circulation episodes, the injected fluid chemical composition is kept constant in the simulation and is not affected by the chemical reactions calculated between the injection and the production well.

4.2.3 Injection temperature impact on the reservoir

Dissolved mineral phases that are close to saturation in the geothermal fluid may precipitate very quickly after a small temperature change. The two minerals with the highest reaction rates in the Soultz system are calcite and amorphous silica. The solubility of the latter is proportional to temperature, whereas the solubility of calcite decreases with increasing temperature. As mentioned earlier, one of the major threats to the durable exploitation of the geothermal system is amorphous silica scaling reducing the injectivity index of the injection wells, and, for a given silica concentration, the lower the injection temperature, the more likely amorphous silica will precipitate.

To assess the risk of scaling in the injection wells, two injection temperatures have been simulated and the results compared. Figure 13 shows the effect of fluid injection on the reservoir temperature after 5 and 10 years of circulation in a reservoir set initially at 200 °C. Two injection temperatures are considered, 50 and 65 °C. Cooling is significant only in the first hundred meters after five years. The 15 °C difference in the injection temperature does not affect the reservoir in a significant manner. After 10 years of circulation, the cooling effect is clearly visible beyond 120 m. In conclusion, with respect to reservoir temperature, the selection of injection temperature is not significant on the long-term. However, the reservoir cools significantly around the injection well upon continuous injection after ten years, but given the important size of the reservoir deduced from tracer tests and the low recycling of the injected fluid (Sanjuan et al., 2010), this cooling may likely not affect significantly the temperature of the geothermal fluid in the production well GPK2 and, subsequently, the energy output of the EGS system.

If the reservoir temperature is only moderately affected by the injection temperature in the range usually encountered at the outlet of the Soultz heat-exchangers, the water-rock interactions are much more prone to change with temperature variations. Figure 14 shows the abundance of amorphous silica around the injection well after 5 and 10 years of fluid injection at 50 and 65 °C. The difference between the two injection temperatures reaches a factor three in the abundance of precipitate amorphous silica. In both cases, however, the total amount of precipitated amorphous silica remains small and does not affect significantly the permeability of the reservoir. Additionally, the length of fracture where amorphous silica deposits occur does not exceed 10 m from the injection well, even after ten years. The low amount of deposition of this mineral according to the numerical simulation tends to show that it is rather unlikely to cause any serious problems for long-term exploitation of the Soultz system.

The bottom-hole temperature in GPK1 is 165 °C, whereas it was measured at 200 °C in the three deep wells. Some simulations have been run to observe a potential difference in chemical reactions between GPK1 and GPK3 and their different temperatures. The cooling induced by the fluid injection is such that the initial reservoir temperature—within the considered range—has a significant impact on the reservoir temperature around the fracture only during the first weeks of circulation. At the scale presented in Figure 14, the curves representing an initial reservoir temperature of 165 °C are perfectly superimposed on the curves of 200 °C.

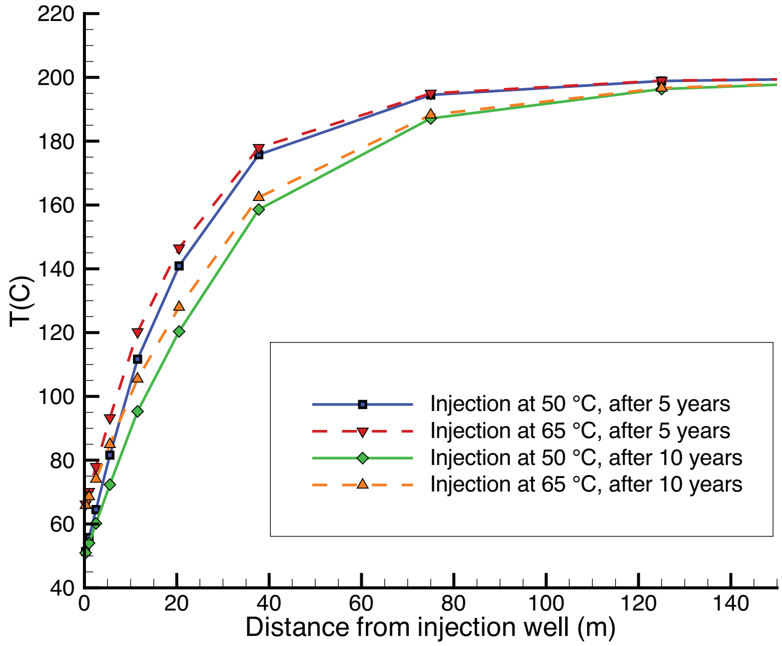

Figure 13: Cooling effect of the injected fluid in the reservoir. Comparison between two injection temperatures (50 and 65 °C) after 5 and 10 years of continuous fluid injection. Initial reservoir temperature: 200 °C.

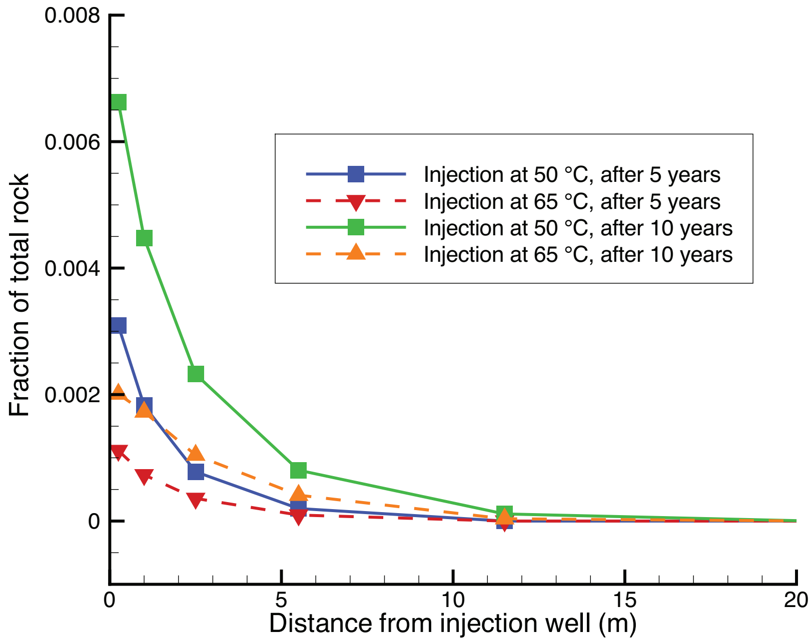

Figure 14: Abundance increase of amorphous silica in the reservoir around the injection well with injection temperatures of 50 and 65 °C, after 5 and 10 years of continuous injection, respectively.

4.2.4 Permeability evolution

The volume changes of the mineral phases impact the permeability of the simulated fracture and will ultimately determine the sustainability of the production scheme. The minerals that are potentially dissolving in the system are mainly calcite, mainly in the vicinity of the injection wells because of cooling, dolomite and K-feldspar. In the results of the simulations performed with TOUGHREACT, the permeability increases clearly in the first few meters of the fracture, gets closer to the initial permeability after about 10–20 m, and increases again slightly up to 100 m from the injection well (Figure 15). This latter permeability increase extends always further during the simulated years, but the amplitude of the increase is too small to be really significant, even after 5 years.

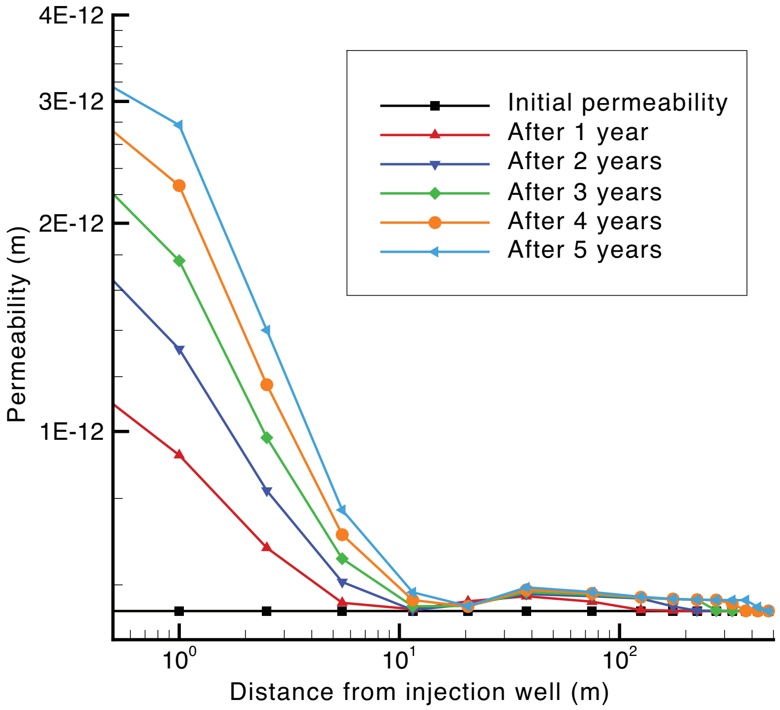

Figure 15: Permeability evolution in the fracture simulated with TOUGHREACT between 0 and 5 years of fluid circulation.

The permeability increase is mainly a consequence of calcite dissolution close to the injection well. Figure 16 shows the volume fraction variation calcite mineral with reference to the undisturbed reservoir rock along the simulated fracture after 1, 2, and 5 years of fluid injection at 65 °C. No variation in mineral abundance is therefore represented by the value “0” on the Y-axis. The “bumpy” appearance of the curves is a consequence of the relatively low spatial resolution and should be smoothed out in a model containing more grid blocks. In the first meters of the fracture, calcite is progressively dissolved with time until all of the 5 % of the reservoir rock represented by that mineral has been exhausted. The dissolution front then progresses slowly away from the injection well and reaches almost ten meters after five years of fluid injection. After the zone of calcite dissolution, some calcite precipitation takes place in the fracture up to almost 100 m, but the amounts remain small, well below 1 % of the total rock after 5 years.

The other minerals play only a minor role in the control of the rock permeability as the mineral mass dissolved or precipitated ranges between one and many orders of magnitudes below that of calcite. As an example, the mineral fraction variations of quartz are shown in Figure 17; the variation in mineral volume is about one order of magnitude smaller than that of calcite. No important dissolution or precipitation is observed in the immediate vicinity of the injection well, whereas some quartz does precipitate after a few meters and up to about 100 m. At the point of maximum precipitation after 5 years, quartz increases its volume fraction by 0.2 %, which is negligible in terms of porosity and permeability. The precipitation zone is followed, after 100 m, by some quartz dissolution in the fracture, but in even smaller amounts.

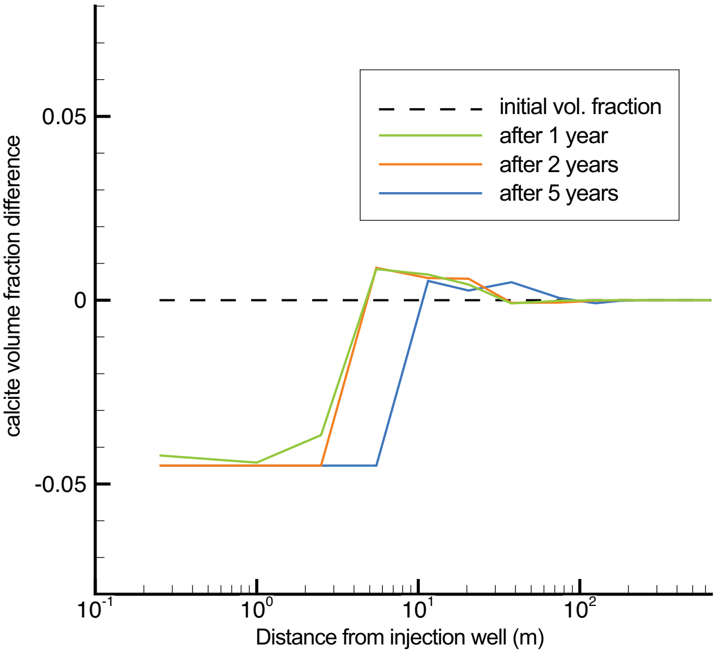

Figure 16: Calcite abundance variation in volume fraction along the simulated fracture after 1, 2 and 5 years of injection at 65 °C.

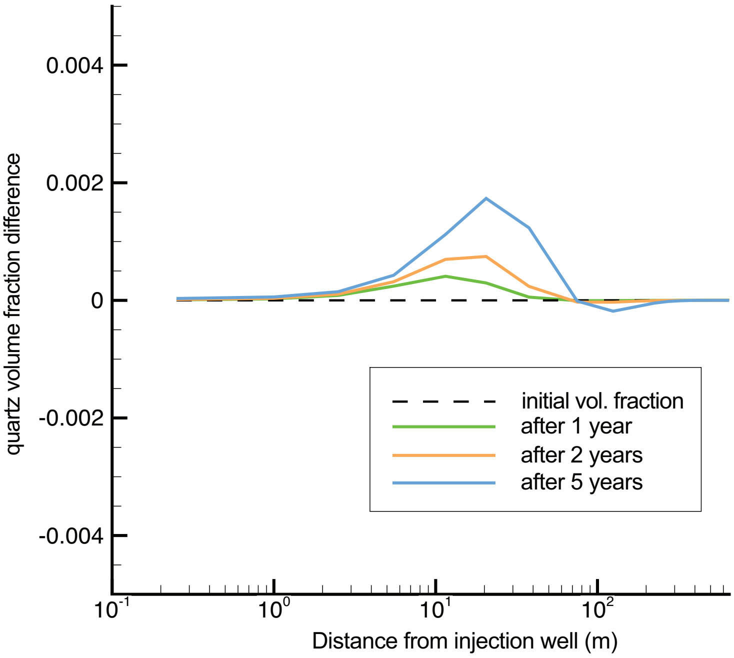

Figure 17: Quartz abundance variation in volume fraction along the simulated fracture after 1, 2 and 5 years of injection at 65 °C.

Amorphous silica, dolomite and K-feldspar are not shown here, but the volumes considered are even smaller than for quartz, by several orders of magnitude. Amorphous silica tends to precipitate slightly in the first 1–2 m from the injection well but no precipitation/dissolution seems to take place beyond 3 m. It cannot dissolve further in the fracture, as it is not part of the initial minerals present in the reservoir rock in the model input. Amorphous silica precipitation is expected close to injection well, since its solubility decreases quickly when the temperature drops, and the model tends to confirm this.

What the latest simulations of fluid circulation within one fracture between the two wells show, is a tendency of permeability improvement close to the injection well due to calcite dissolution. This can be extrapolated to the whole fractured zone hosting fluid flow between injection and production wells. Some mineral precipitation do take place, according to simulation results mainly as calcite and quartz, a few meters away from the injection well and extending beyond 100 m, but the mass of mineral remains small. It should be mentioned as well that the model considers that the entire injected fluid follows a single path towards the production well. However, the injected fluid is mixed to a large volume of fluid and only a fraction of it returns to the production well (see for instance the considerations on reservoir temperature and size in Section 5). As a concluding remark, the numerical simulations performed in the frame of this project do not allow to predict a decrease of reservoir performance due to mineral precipitation.

These results come very close to the conclusion of simulations previously made with FRAChem, and the behaviour of most minerals approached the tendencies we do observe in this report.

5 Chemical behaviour of the Soultz reservoir

5.1 Introduction

The chemical composition of the fluid produced and reinjected in the system is of major importance for the operation of the geothermal loop, since inappropriate circulation conditions or the wrong selection of materials can severely limit or even annihilate productivity by favouring scale deposits and/or corrosion. The deposition of scales can occur either in the reservoir, in the vicinity of the well, or in the well and the surface installations, where corrosion can also occur, requiring early cleaning or replacement of affected materials. Hence, careful monitoring of the chemical composition of the liquid phase, gas concentrations and the potential scales should be organized at every stage of the exploration and exploitation of the resource.

At Soultz, the fluid characteristics are monitored in two ways:

- The geothermal brine injected in GPK3 is continuously monitored for temperature, Eh, pH, and conductivity.
- The fluids produced from GPK2 and reinjected after cooling in GPK3 and GPK1 are periodically sampled and analysed for major and trace elements.

Because of the long interruptions of the production from well GPK2 after March 2011 due to technical problems in the LSP pump, the most recent samples collected by the BRGM and presented in this report were collected during the production test performed between November 2009 and October 2010, and during the following circulation period that spanned from January to March 2011. The first production test lasted 323 days and is the longest circulation since beginning of production. The samples were collected in June and July of 2010, after more than 6 months of fluid circulation at flow-rate values close to 18 l s^{-1}.

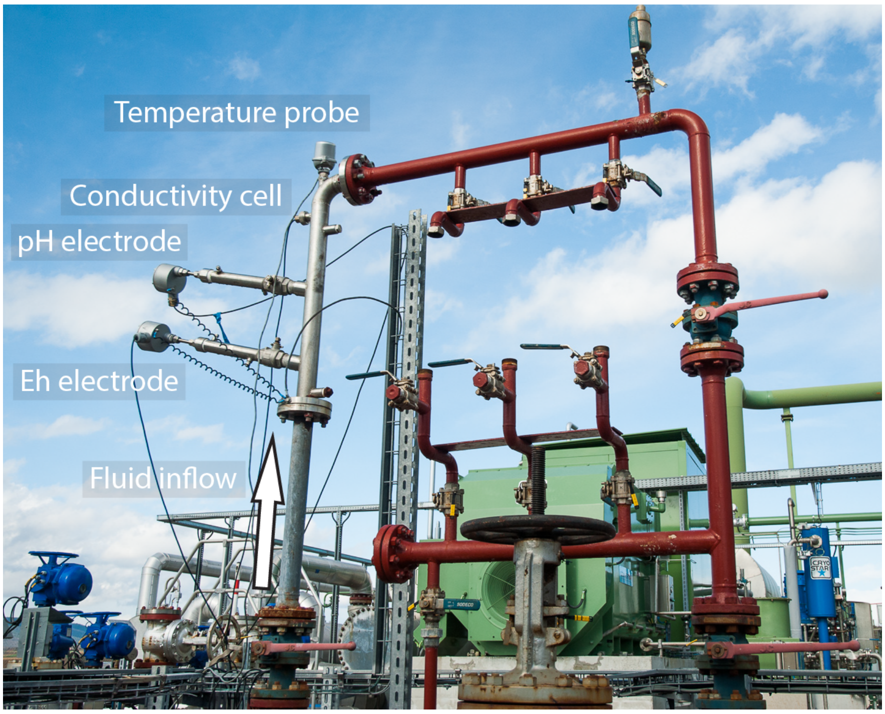

Figure 18: Continuous monitoring skid on the injection pipeline of well GPK3.

5.2 Continuous monitoring of the fluid injected in GPK3

The continuous monitoring of the injected fluid located on the pipeline before GPK3 was setup on a derivative ¾” pipe (as opposed to the main 6” pipe, see Figure 18) and started monitoring temperature, Eh, pH and conductivity on the 10th of March 2010, about one month after the beginning of a production test from GPK2 and reinjection in GPK3. The temperature and pressure in the monitoring pipe were respectively 60–80 °C and 20 bars. After two months of continuous monitoring, the probes showed a black deposit probably of poly-metallic sulphides and oxides. All the probes were later removed and replaced by new ones, but this did not improve the black scaling on the probes, which need to be removed and cleaned at regular interval. The monitoring was further carried out during production tests until October 2011.

The continuous monitoring of conductivity seems globally very unreliable, with inconsistent values even with a regular cleaning and after the replacement of the probe. Eh and pH measurements, however, show interesting results in the first months of non-stop monitoring. Values of -384 mV for Eh and 4.63 for pH were measured in October 2010, not long after the replacement of the probes. These values are considered to be the closest to the deep original brine ever measured (Sanjuan, 2010). However, after a year of monitoring (September 2010 to October 2011) interrupted by several maintenance periods of the LSP pump, all the probes and the monitoring loop show heavy wear by scale cleaning and corrosion. The main conclusion from this experiment is that a continuous and long-term monitoring of a fluid of such salinity and redox potential is extremely difficult to perform in a reliable way.

5.3 Evolution of chemistry with time

The analyses shown in Table 9 include a selection of fluid samples collected from well GPK2 by the BRGM since the start of fluid production after the well was deepened from 3,900 to 5,000 m in 1999 and up to 2011. Most of the samples were collected using a cyclonic micro-separator constructed by EEIG to allow comprehensive sampling of both liquid and gas phases.

Silica analyses for all samples—except that of 1999—show values that are about half the estimated concentration of 427 mg/l in the native geothermal brine, which corresponds to the equilibrium with quartz at the reservoir initial temperature of 230–240 °C. The low values obtained from sampling at the wellhead are likely a consequence of silica precipitation due the cooling of the fluid during its ascent in the well.

During the drilling phase and subsequent reservoir stimulation, very large amounts of fresh (dilute) cold water were injected in the wells and became mixed with the original reservoir fluid. The brine samples collected from the different wells all seem to be diluted to some extend by the injected fresh water. Considering the native brine of the reservoir, the fraction of injected water in the sampled fluid represented about 5 % during the first production tests. Figure 19 shows that chlorine, sodium and magnesium have concentrations that are close to what is considered the “native brine” of the reservoir (Sanjuan, 2010, shown as “NGB” in Table 9 and by the dotted line in Figure 19). The conservative behaviour of Cl allows us to conclude that in 2011, the proportion of injected water in the collected samples is down to 2–3 %. Sodium and magnesium are more likely to have equilibrated with reservoir rock minerals, but both anyhow show values that are close to NGB.

Table 9: Selection of main chemical compounds of waters sampled from production well GPK2 between 1999 and 2011. NGB stands for "Native geothermal brine" and represents, by calculation, what the native brine could be in the undisturbed reservoir (Sanjuan, 2010).

Fluid sample	Sampling date	Cond. at 25 °C (mS cm^{-1})	pH (at temp.)	Na (g l^{-1})	K (g l^{-1})	Ca (g l^{-1})	Mg (mg l^{-1})	Cl (g l^{-1})	SO_4 (mg l^{-1})	Alk. (meq l^{-1})	SiO_2 (mg l^{-1})
GPK2-99-S2	26.11.99	126	5.43 (20.0 °C)	26.8	2.88	6.65	75	57.8	171	6.6	409
GPK2-02-P71	24.04.02	97	5.58 (20.0 °C)	23.5	2.77	5.02	124	46.2	150	5	262
GPK2-03-P42	09.07.03	78	5.67 (20.0 °C)			3.46		32.6		2.1	212
GPK2-05-P149	22.11.05	110	5.39 (20.0 °C)	22.9	2.59	6.1	106	49.3	157	2.3	255
GPK2-10-E3	05.05.10	130	6.90 (15.1 °C)	26.2	3.26	6.88	136	57.7	185		221
GPK2-11-E4	22.02.11	129	5.50 (40.1 °C)					59.5		1.48	226
GPK2-11-E11	09.08.11	109	5.21 (22.2 °C)					55.1		3.31	227
GPK2-11-E37	19.10.11	127	5.10 (22.6 °C)					56.7			
NGB		135	5.00 (25.0 °C)	27.5	3.25	6.9	125	59	190	5	427

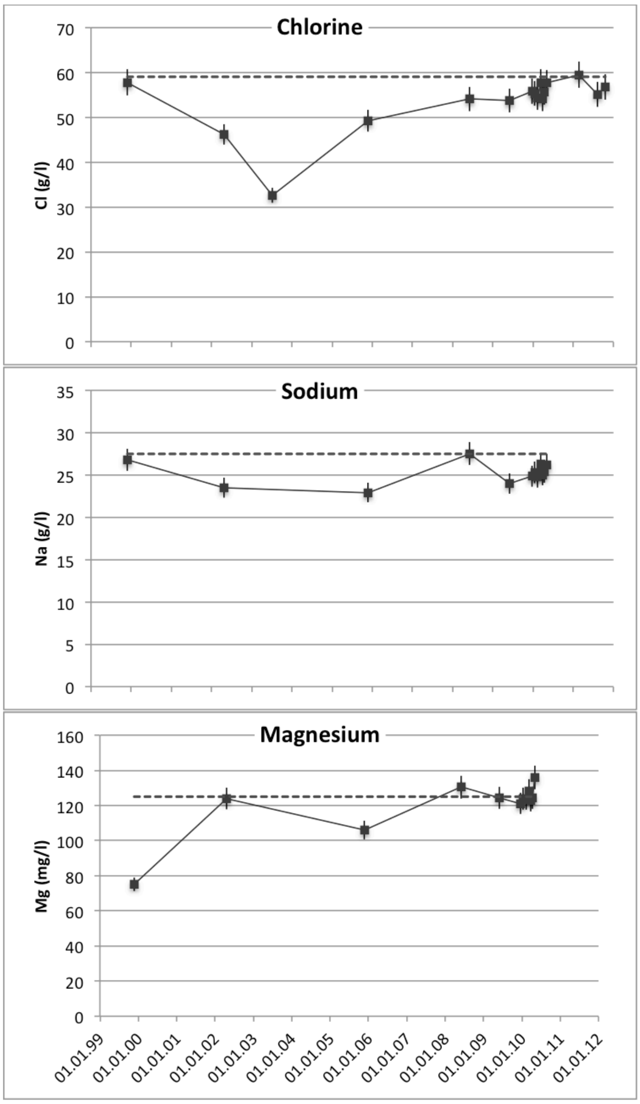

Figure 19: Evolution of chlorine, sodium, and magnesium in waters sampled from production well GPK2 between 1999 and 2011. The dotted line represents the Native Geothermal Brine (NGB). Error bars represent an uncertainty of 5 %.

5.4 Gas concentrations

Samples of free gas were collected by the BRGM at various times of fluid circulation tests using a micro-separator at the wellhead of the GPK2 and a selection of values is shown in Figure 20. The analyses were performed at GFZ German Research Centre for Geosciences for the 1999 sample and by BRGM for the other samples. The relative analytical error is about 5 %, but gas concentrations are very sensitive to sampling conditions (extension of the phase separation, separation pressure, etc.), leading to some discrepancy in the results.

However, we can observe a strong variation in the 2010–2011 samples, as compared to the earlier samples of 1999 and 2005. The later samples show CO_2 concentrations above 80 % v/v while earlier samples showed values closer to 60 % v/v. Since the gases are measured as relative concentrations, the other gases measured, N_2, H_2, CH_4, and He show an important decrease of their concentrations in the last years. At the same time the gas to liquid ratio increased from 13–38 % v/v up to 75–107 % v/v in 2010–2011. Carbon dioxide is therefore mainly responsible for this increase of the gas to liquid ratio. Unfortunately, these numbers could not be confirmed in 2012 due to important down time of the geothermal loop that hindered any sampling campaign, and we should therefore be careful before drawing to many conclusions from these gas concentration changes.

Boiling in the reservoir would rather lead to an even stronger increase of the concentration of the least soluble gases compared to CO_2, in particular N_2 and He, unless extensive boiling had completely degassed the reservoir fluid from inert gases while allowing reactive gases to equilibrate with the primary and secondary minerals. However, in this case the reactive gas CH_4 would also equilibrate and its concentration trend would follow that of the CO_2. The increase in the mass of CO_2 output in the fluid could rather be linked to calcite precipitation, where the following reaction

$$\mathrm{CaCO_3} + \mathrm{H_2O} + \mathrm{CO_{2(g)}} = \mathrm{Ca^{+2}} + 2\mathrm{HCO_3^-}$$

moves to the left. Numerical simulations show that calcite has indeed the tendency to precipitate in the vicinity of the production well. However, calcite precipitation at large scale in the fluid close to the production casing would be followed by a measurable decrease of calcium concentration in the discharged fluid.

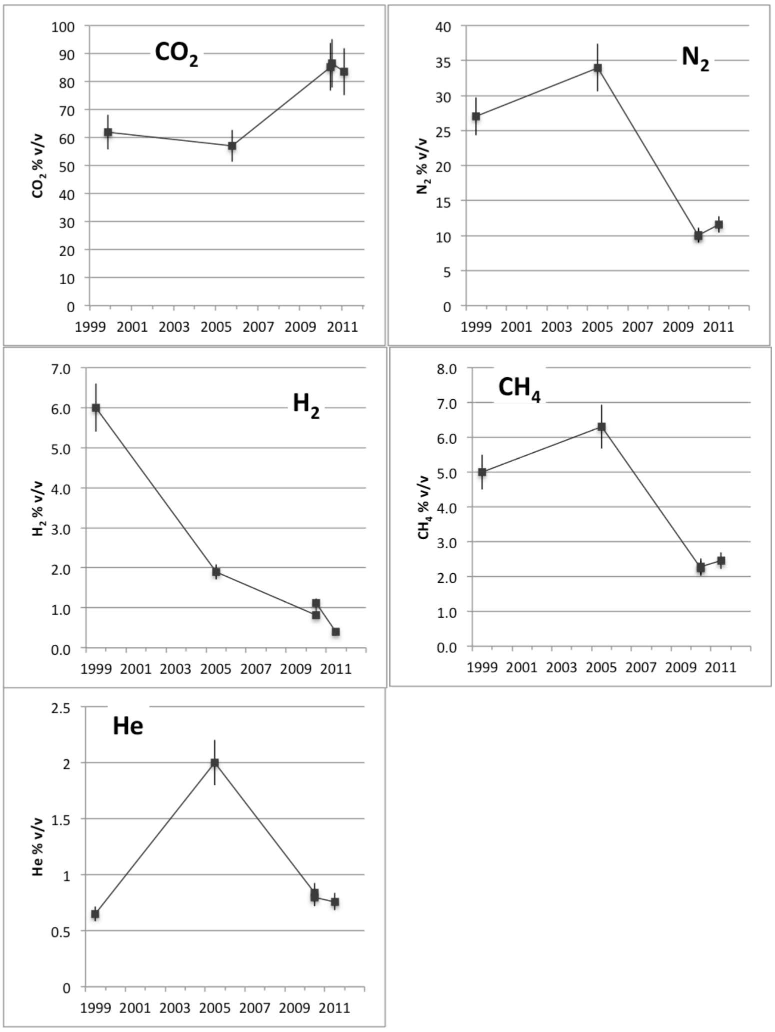

Figure 20: Gas concentrations in percent by volume, measured in the separated gas phase from the discharging fluid of well GPK2 in 1999, 2005, 2010 and 2011. Error bars represent an analytical uncertainty of 5 %. The values plotted here are presented in Appendix II.

5.5 Reservoir and exploitation temperature conditions

During the period 2009–2010, the production temperature of GPK2 has been rather stable with time, between 160 and 164 °C. The temperature measured at the bottom of the three deep wells is close to 200 °C, which means that the fluid is cooled during its ascent and/or mixed with cooler fluids. Two factors can be the cause of mixing: potential casing leaks and connection with large sub-vertical faults bringing fluids from the shallow reservoir. The water injected in GPK1 and GPK3, after having lost some of its heat in the heat exchangers, has a temperature of 55 to 75 °C, depending on the on how the production loop is set (flow-rates on the three wells, respective temperatures, thermal output in the heat exchangers, etc.). Several down-hole temperature logging have been carried out in the different wells in order to understand potential leakages of the wells, convection cells in the reservoirs, and hydraulic connections between wells. A down-hole temperature log was recorded in GPK3 in 2005, after two months of injection at 15 $l\,s^{-1}$ and 55 °C, which showed a sharp temperature increase of about 15 °C at a depth of 1,800 m (Schellschmidt, 2011). This important heat input was suspected to come from the production well GPK2. In 2006 and 2010, two further logs showed even stronger heat inputs, at about 1,620 m and 1,815 m. The calculated heat input to the injected fluid of GPK3 corresponds to a thermal power of 0.9 MW. A cooling is indeed observed in GPK2 at similar depth, confirming the hypothesis of a hydraulic connection between the two wells, which are only distant of 35 m at that depth. Dezayes (2010) observed the occurrence of fractured zones at these depths, further confirming the possibility of the hydraulic connection linking the two wells. This connection is the main influence that GPK3 has on the fluid production regarding temperature.

During the circulation tests in 2009–2010, the fluid temperature produced from GPK2 was relatively stable at 160–164 °C with a low injection rate in GPK1. However, as mentioned in section 4.1, an increase of the injection flow-rate in GPK1 from 2 $l\,s^{-1}$ up to 7.5 $l\,s^{-1}$ in February 2011 led to an average temperature drop in the GPK2 fluid of 5 °C, from 164 °C down to 159 °C (Melchert, 2010). After this drop, the temperature in GPK2 has remained stable. Similarly, at the start of the injection in GPK1 in 2010, a small temperature drop was observed in the production well. We can therefore conclude that there is a hydraulic connection between GPK1 and GPK2, but no thermal breakthrough. At the time when GPK4 was also used as a producing well, no hydraulic connection had been observed between that well and GPK1.

5.6 Geothermometers

Calculations of temperatures by geothermometers were previously performed by Pauwels et al. (1993) and Aquilina et al. (1997) on the fluids of the upper reservoir down to a depth of 3,500 m, and by Sanjuan et al. (2010) for the fluids collected from the deeper reservoir.

As mentioned in section 5.3, silica seems to precipitate during the ascent of the fluid in the production well and the concentrations that are measured upon sampling are about one half of the concentrations that are expected at equilibrium with the estimated reservoir temperature at 230–240 °C. Therefore the geothermometers based on dissolved solids have been calculated using concentrations in samples collected shortly after the deepening of well GPK2 in 1999. A consistent temperature range of 220–240 °C is obtained using various classical chemical geothermometers, which is slightly higher than the 200 °C measured at the bottom of the three deep wells.

6 Guidelines for geochemical management of the fluid during the exploitation of the Soultz EGS reservoir

6.1 Introduction

These guidelines are based on the knowledge of the formation fluid of the Soultz shallow and deep reservoirs, and on the numerous experiments carried out during the production/injection tests of the development phase as well as the exploitation phase.

The efficiency of the exploitation of an EGS geothermal plant is strongly correlated to the energy required for pumping a given flow-rate of geothermal fluid from the production wells and into the reinjection wells, and to the frequency and cost of maintenance operations.

The factors controlling these parameters are the permeability of the reservoir in the vicinity of the wells, the quality of the fluid, the temperature and pressure changes during the transport and heat extraction of the fluid, and the design of the geothermal loop, including the selection of materials for the well casings, pipes, heat-exchangers, filters, etc. The quality of the fluid is a key parameter that has to be taken into account since the first exploration phases as it plays the head role in the control of each of the above listed parameters. The main characteristics of the fluid produced from the deep wells at Soultz-sous-Forêts is its high salinity (90–100 g l^{-1}), about three times that of see water, which can lead to an important reactivity and subsequent potential corrosion and scaling problems. Corrosion affects the geothermal loop between the production and injection wells, including the well casings, whereas scaling may also affect the reservoir permeability, especially in the vicinity of the wells. Besides, dissolution of secondary minerals coating the reservoir fractures can on the contrary improve the permeability and therefore the productivity or injectivity indices.

The various parts of the geothermal system where problems related to the chemistry of the geothermal fluid are described below. Figure 21 presents a schematic view of the various parts of the system, and Table 10 lists the potential issues in each of the sections and the possible mitigation procedures.

6.2 Fluid production

The long circulation period of 2009–2010 was a good opportunity to observe the behaviour of the reservoir upon production. However, for technical reasons, no water level measurements could be performed in GPK2 in 2010. During the 323 days of circulation, the flow-rate could be maintained at 18 l s^{-1} with no need to increase the long shaft pump frequency.

More detailed measurements could be carried out in 2011 during the two circulation periods. During these production phases the flow-rate was progressively increased from 18 l s^{-1} up to a maximum of 26 l s^{-1}, quickly decreased again to 23 l s^{-1} due to concerning vibration and suspected damage of the LSP pump. This flow-rate increase was led to an increase of particulate material brought to the surface by the fluid. From January to April 2011, 200 kg of cuttings were lifted from GPK2 (Genter et al., 2012) and recovered in the filtering system, showing that the well had not yet been completely cleaned up after drilling. The removal of this material increased the productivity index of the well from 1.2 up to 1.9 l s^{-1} bar^{-1}.

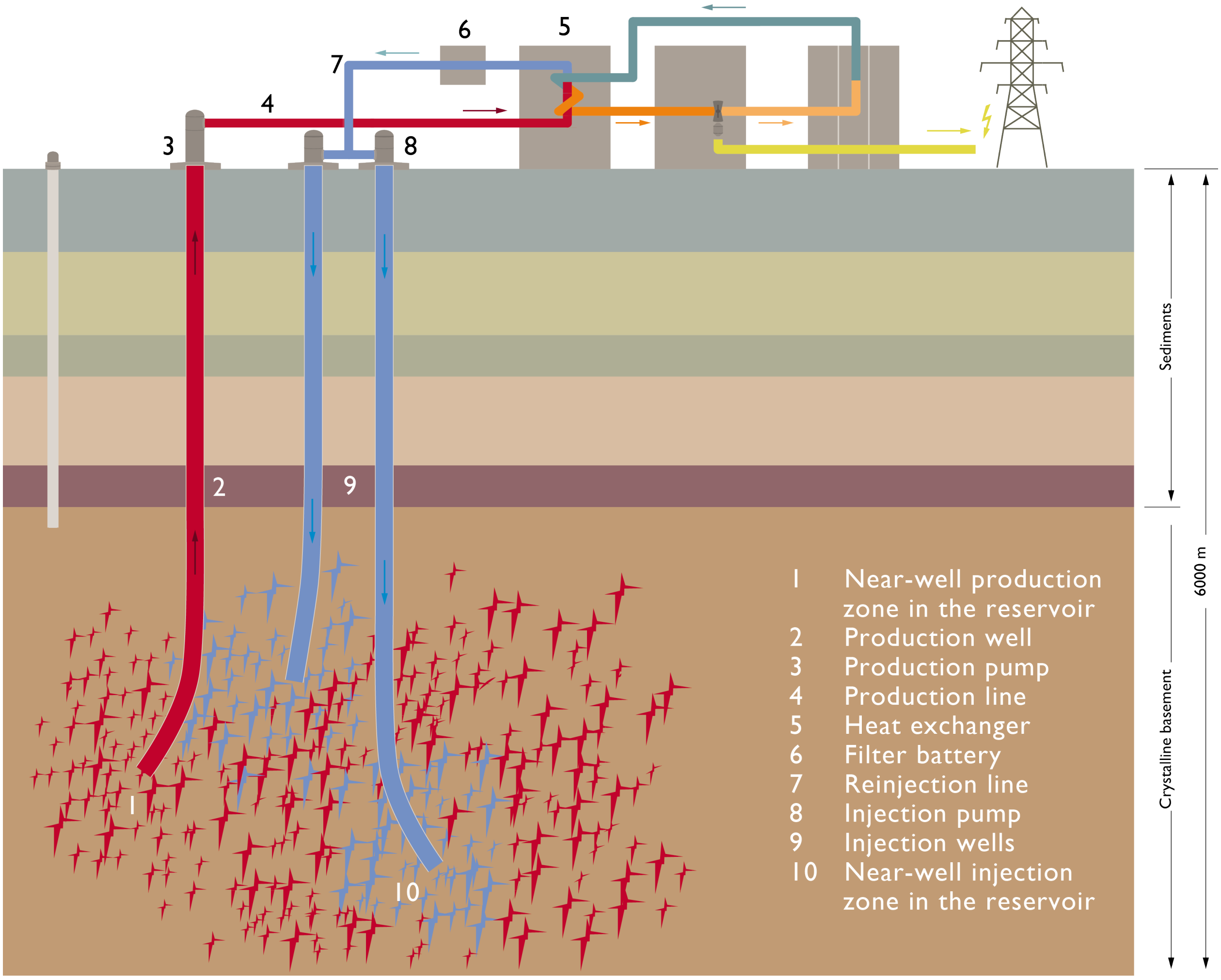

Figure 21: Schematic view of the Soultz geothermal system. Numbers show system parts where potential problems related to geothermal fluid chemistry can occur. (Modified from GEOPOWER Basel)

The pump technology installed in GPK2 does not seem to handle flow-rates above 22–23 l s^{-1} and it seems unlikely that much higher flow-rates will be used in the future. One can only assume that most of the remaining cuttings in the fractures have been removed after the 2011 circulation phases and that no further damage will be caused by particulate material lifted with the fluid.

On a geochemical point of view in the reservoir, the stable productivity over a long period confirms the results of the numerical models, showing that no important mineral precipitation should occur close to the production well. Nevertheless, the low silica concentrations measured at the wellhead tend to indicate that silica scaling is occurring from the flowing fluid in the vicinity and inside the production well. As silica solubility decreases with decreasing temperature, it tends to precipitate upon cooling during the ascent of the fluid in the well and may in the long run contribute to the clogging of well GPK2. Boiling inside the well would further enhance cooling and should therefore be avoided as much as possible by adjusting the fluid pressure at the wellhead. As mentioned above, the optical observation of the well casing on the top most 500 m did show some scaling but obviously no important silica scaling layers.

Table 10: Description of the physical and chemical processes, and the potential issues that are prone to occur in the various parts of the geothermal system. The important parameters to monitor and proposed mitigation measures are also shown. Numbers in the first column correspond to the parts in Figure 21.

Nb	Location on the geothermal loop	Physical and geochemical processes	Potential problems	Monitoring parameter	Mitigation measures
1	Near-well production zone	- Boiling - Degassing	- Scaling	- Well productivity	- Control production flow rate to limit depressurization - Reservoir stimulation
2	Production well (casing and wellhead)	- Cooling - Boiling - Degassing	- Scaling (calcite, amorphous silica, etc.) - Casing corrosion	- Well productivity	- Control pressure in the well to avoid boiling - Well cleaning
3	Production pump (LSP or ESP)	- Cavitation - Corrosion of electrical or mechanical parts	- Mechanical erosion, pump breakdown	- Periodic control of the pump	- Pump technology and material selection
4	Production line	- Degassing - Cooling	- Scaling (calcite, barito-celestine, sulphides, oxides)	- Periodic visual control - Fluid chemistry (pH, Fe, SiO_2, Cl, etc.)	- Keep pressure above degassing - Ev. inhibitor injection or coating
5	Heat exchanger	- Cooling - Local T and P variations	- Corrosion - Scaling	- Periodic visual control - Radioactivity measurement	- Inhibitor injection or material coating
6	Filter battery	- Local T and P variations	- Scaling - Corrosion	- Periodic visual control	- Inhibitor injection or material coating
7	Injection line	- Cooling	- Scaling - Corrosion	- Periodic visual control - Fluid chemistry (pH, Fe, SiO_2, Cl, etc.)	- Control of injection temperature - Inhibitor injection
8	Injection pump	- Local T and P variations	- Chemical and mechanical corrosion	- Periodic visual control	- Pump technology and material selection
9	Injection well (wellhead and casing)	- Progressive T and P increase	- Scaling (silica, corrosion products, etc.) - Corrosion	- Well injectivity	- Control injection temperature - Inhibitor injection
10	Near-well injection zone	- Temperature increase of the fluid - Cooling of the reservoir	- Mineral precipitation and permeability reduction	- Well injectivity	- Control injection temperature - Inhibitor injection

Fluid degassing is potentially one of the most harmful processes in terms of mineral precipitation. Carbon dioxide in solution is mainly present as weak acids, HCO_3^- and H_2CO_3. Its removal from the liquid phase by simple degassing or boiling of the fluid raises pH, which brings calcite to over-saturation. The kinetics of the reaction is extremely fast and has been observed in many geothermal fields were CO_2 degassing has led to the precipitation of large amounts of calcite.

6.3 Surface installations

The surface installations at Soultz do host some slow scaling processes, whose products are mainly barito-celestine, magnetite, galena, pyrite, sphalerite, illite, and quartz (Genter et al., 2012). Sulphide mineral precipitates are observed in some locations of the surface loop, while the H_2S concentration in the fluid is below the detection limit. This scaling occurs mainly on the cold side of the loop, after the heat exchanger on the injection line, and also inside the injection wells. A survey of GPK1 with an optical camera down to a depth of 500 m showed the presence of limited and non-differentiated deposit on the well casing (Scheiber, 2012).

The main issue with scaling encountered in the surface installation at Soultz so far is linked to radioprotection. The geothermal fluid circulating in the relatively uranium rich crystalline basement contains traces of radioactive elements, which can be trapped in scale minerals. In particular, barium-bearing minerals can exchange barium ions by ^{226}Ra, and ^{210}Pb can be present in galena. The presence of these scales in the various parts of the power plant loop brings working safety problems and the scales that are removed need to be treated as low-radioactivity materials.

In order to limit the deposition of the scales, the use of inhibitors has been investigated (Scheiber, 2012). Several laboratory experiments were performed using brine samples collected on-site and three commercial phosphonic acid inhibitors. All three inhibitors limited the formation of barium/strontium sulphates, but only two of them were also effective at hindering the formation of oxides and sulphides and will therefore be tested on-site by a continuous injection operation and subsequent monitoring of scaling formation and fluid chemistry.

Calcite scaling is a frequent problem in geothermal power plants, often linked to CO_2 degassing of the fluid. The lost of carbon dioxide rises the pH, leading to calcite over-saturation. At Soultz, the pressure in the upper part of the production well and in the surface loop is maintained around 18–20 bars to avoid degassing. This method proves to be efficient with time, as no significant calcite scaling has been observed after the circulation phases.

Corrosion experiments have been conducted both on-site and in laboratory. A corrosion pilot has been setup in the monitoring skid on the line of the injection well GPK3 (see Figure 18). The results showed some scaling, but also pitting corrosion under the scales (Baticci et al., 2010). Laboratory experiments conducted by Müller et al. (2010) showed some corrosion on carbon steel samples. The coatings mentioned above may also prove effective as protection against corrosion.

6.4 Fluid injection

In many high enthalpy geothermal fields around the world, fluid reinjection is limited by the declining injectivity of injection wells. Often encountered high silica concentration lead to important scaling and clogging of wells, due to amorphous silica and/or chalcedony precipitation. At Soultz, the injectivity varies between wells and the pressure needed for injection is higher in GPK3 than in GPK1, were injection flow-rates up to > 13 l s^{-1} can be obtained using gravity only (Genter et al., 2012). On the contrary, a wellhead pressure of 18.5 to 20 bars is needed to reach a flow rate of 9 l s^{-1} in GPK3. The two biggest drawbacks of a high injection pressure are the increased risk of induced seismicity, and the decrease of the efficiency of the power plant because of the electrical power consumption increase by the injection pump.

Numerical simulations show that amorphous silica tends to precipitate in the fracture network close to the injection wells, with, however, relatively low reaction rates. The reaction rates of calcite are about one or two orders of magnitude higher than that of amorphous silica and therefore calcite dissolution and precipitation is mainly controlling the permeability of the reservoir. The result is that the injection of cooler brine dissolves important amounts of calcite around the well, which improves the injectivity of the well, and which is only balanced to a small extend by silicate mineral precipitations, mainly as amorphous silica. Quartz and alumino-silicate minerals only play a secondary role in terms of volumes dissolved or precipitated.

On the long run, when calcite minerals along the fractures have been extensively dissolved around the injection wells, amorphous silica precipitation may take over the porosity increase and start reducing the permeability in a way that could affect the injectivity of the well in the long run. Even though this may happen only after many years, some chemical stimulation would then be required to regain the lost permeability.

The injection temperature, within the 60–80 °C range used at Soultz, has only a limited impact on the water-rock interactions in the reservoir and can therefore be adapted to the needs of power production and the control of corrosion and scaling in the geothermal loop. However, considering an average silica concentration of 230 ppm in the fluid, amorphous silica becomes over-saturated at temperatures below 66 °C. The injection temperature during power production should therefore stay in the range 65–75 °C so as to limit amorphous silica scaling in the reinjection line and wells.

6.5 Chemical monitoring

The evolution of the fluid chemistry along the whole geothermal loop gives an excellent insight on the occurrence of some geothermal processes that can potentially severely impede the exploitation of the system. A complete sampling (gas and liquid phases) at the wellhead using a micro-separator gives a feedback of the reservoir response to fluid extraction, as physical and geochemical processes occurring in the near-well reservoir (boiling, scaling, etc.) will significantly affect the discharged fluid chemistry. Table 11 summarizes the fluid chemical monitoring program that will provide a sufficient control of the system while keeping analytical costs at a minimum. Some parameters are currently monitored at close interval during the circulation phases. However, during long-term exploitation of the geothermal installation, a routine control of basic physical and chemical parameters (temperature, pressure, flow-rate, and electrical conductivity) can be carried out on a weekly basis both on the production and the injection line. On a quarterly basis, the chemistry should be checked by measuring the concentration of some key components of the geothermal fluid on both hot and cold lines (Na, Cl, SO_4, dissolved CO_2, and SiO_2). A complete sampling of both the gas and liquid phases collected using a micro Webre separator close to the production wellhead should be performed at least once a year to get a thorough control of the evolution of the system upon long-term production and injection. This sampling should include major dissolved elements and selected trace elements, water isotopes, tritium, gas-to-liquid ratio, and gas phase composition (Table 12). These analyses allow for detailed calculations of water-rock interactions in the reservoir and their modification with time, but may also give an insight on corrosion and scaling in the parts of the system that are not easily checked visually, like the well casing.

In case of significant changes in the routinely measured parameters, a more comprehensive sampling should be organized in order to identify the cause of the variation.

Table 11: Summary of monitoring program. Numbers in the first column correspond to the parts as shown in Figure 21.

Nb	Location	Parameters	Frequency
4	Production line	- Temperature - Pressure - Flow-rate - Electrical conductivity	Weekly
		- Na, Ca - Cl, SO_4 - Dissolved CO_2 - SiO_2	Quarterly
		- Major and selected trace components - Gases - Isotopes (δ^2H, $\delta^{18}O$, ^3H)	Yearly or biannually, using a micro-separator
7	Injection line	- Temperature - Pressure - Flow-rate - El. conductivity	Weekly
		- Na, Ca - Cl, SO_4 - Dissolved CO_2 - SiO_2	Quarterly
6	Filter battery	- Analysis of scale minerals	Yearly

Table 12: Chemical components and isotopes that should be analysed during the yearly or biannually chemical monitoring of the geothermal fluid at Soultz.

Type or phase	Parameters and components
Physical parameters	T, P, pH, Eh, electrical conductivity, gas-liquid ratio, flow-rate
Major dissolved components	Na, K, Mg, Ca, B, CO_2, SiO_2, H_2S, SO_4, Cl, Br
Dissolved trace elements	Li, Ba, Ra, Ti, Cr, Mn, Fe, Ni, Cu, Zn, Cd, Hg, Al, Pb, As, I
Gas phase	H_2, CO_2, CH_4, N_2, O_2, H_2S, He, Ar
Isotopes	δ^2H (H_2O), $\delta^{18}O$ (H_2O), ^3H

7 Meetings and publications during this project phase

7.1 Published articles and abstracts

During the period of the report, an article summarizing the results of the numerical simulation of the chemical stimulation performed at Soultz was published in Comptes Rendus Geoscience.

A paper was also accepted at the World Geothermal Congress held in Bali in 2010, and a short abstract was accepted at the Soultz Geothermal Conference in 2011.

Below is a list of the most recent publications, while Appendix III lists the publications of the Centre for Hydrogeology and Geothermics regarding the Soultz EGS project in the field of geochemistry.

- Portier S., and Vuataz F.-D., 2010. Developing the ability to model acid-rock interactions and mineral dissolution during the RMA stimulation test performed at the Soultz-sous-Forêts EGS site, France. Comptes Rendus Geoscience, 342, 668-675.
- Portier S., and Vuataz F.-D., 2010. Modelling Acid-Rock Interactions and Mineral Dissolution During RMA Stimulation Test Performed at the Soultz-sous-Forêts EGS Site, France. Proc. World Geothermal Congress 2010, 25-29 April 2010, Bali, Indonesia.
- Giroud N., and Vuataz F.-D., 2011, Reactive transport modelling of a one-year fluid circulation in the Soultz EGS reservoir. Soultz Geothermal Conference, Soultz-sous-Forêts, October 2011.

7.2 Meetings

The on-going work on FRAChem was presented at several meetings during the time covered by this report. The meetings are listed below:

- Meeting "EGS: Current state of understanding and future research” funded by the Swiss Federal Office of Energy and held in Basel on March the 30th 2010.
- Kick-off meeting of the Phase III, “Scientific and Technical Monitoring of the Soultz Power Plant”, held in Kutzenhausen on March the 31st 2010.
- World Geothermal Congress 2010 held in Bali April 25–30th 2010, with an extended abstract and a poster entitled: “Modelling acid-rock interactions and mineral dissolution during RMA stimulation test performed at the Soultz-sous-Forêts EGS site, France”
- Soultz Phase III annual meeting held in Kutzenhausen on November the 30th 2010
- Soultz Geothermal Conference, Soultz-sous-Forêts, October 2011.

8 Summary and recommendations

8.1 Summary of the main results

This report closes the third research phase carried out at the University of Neuchâtel on the Soultz-sous-Forêts enhanced geothermal system. This phase has followed closely the operation start of the pilot power plant in 2008 and several forced circulation periods, of the geothermal loop, including the longest circulation ever carried at Soultz. Three wells are used during most circulation phases—one production well and two injectors.

The current research phase has been focussed on numerical models of thermal, hydraulic and chemical processes in the reservoir, applied to chemical stimulations, long-term behaviour of the reservoir, and the enhancement of the modelling tool FRAChem. Additionally, this report provides some guidelines on the geochemical management of the geothermal system in order to limit and control issues linked to the quality of the fluid like corrosion, scaling in the wells and surface installations, as well as permeability reduction in the reservoir.

The fluid at Soultz, in regard to its very high salinity close to 100 g l^{-1}, has not caused any serious damages to the geothermal system. The productivity and injectivity of the wells has remained stable—or has even increased, and the total mass of mineral precipitates in the surface installation is low. However, as the latter does bring some concerns for working safety conditions (radioactivity of the deposits), several actions are presently investigated to deal with this issue, like the injection of a scale inhibitor and the selection of a material coating.

Well GPK4 was chemically stimulated in 2006 in order to improve the permeability of the reservoir, and the estimated result is an improvement of the injectivity index of 35 %. The code FRAChem, which was specifically developed at the University of Neuchâtel for the Soultz geothermal system, was modified to include the acids HCl and HF which were used as dissolution agents in GPK4. The results of the numerical models give an insight of the minerals dissolved in the stimulation process and are consistent with the estimated amounts of dissolved minerals. According to numerical simulations, the porosity increases from 10 % up to 17 % close to the wellbore and the affected zone extends up to 40 m from the well.

The development of FRAChem at the University of Neuchâtel started in 1998 and the code has been constantly enhanced until today. In the period covered by this report, an import update and bug tracking work has been carried out on the program. The executable version of the code will allow the user to perform geothermal fluid circulation simulation on the Soultz reservoir and obtain information on the water-rock interactions and their effect on the porosity and permeability of the reservoir.

During the period covered by this research program, the circulation scheme of the Soultz geothermal loop was modified, following the breakdown of the electro-submersible pump in well GPK4. In addition to the injection in well GPK3, the cooled fluid was also injected in GPK1 in order to reduce the amount of pumping needed for reinjection and limit the risk of induced seismicity. A more than 10 months long circulation test with stable production parameter gave a good opportunity for a geochemical survey of the fluid. The sampling and chemical analyses performed by the BRGM show concentrations that are mostly stable in time for the major chemical components in the fluid phase. Compared to samples collected at the beginning of fluid production from the deeper reservoir, the fluid composition seems to become closer to what is considered as the undisturbed initial reservoir brine. However, the gas concentration in the total fluid discharged has significantly increased, in particular for carbon dioxide, and may be linked to calcite precipitation in the vicinity of the production well. Additionally to the relatively stable chemical composition, no significant temperature drop has been observed in the produced fluid. There is nevertheless a temperature decrease of a few degrees-C proportional to the flow-rate of fluid injected in GPK1, proving the existence of a hydraulic link between wells GPK1 and GPK2.

Numerical simulations of fluid flow in a simplified model of the reservoir show important calcite dissolution in the vicinity of the injection well, up to the complete dissolution of the initial concentration of that mineral in the reservoir rock. As a result, the permeability of the reservoir increases in that area. Calcite precipitates again further in the reservoir, but in much smaller quantities. The other minerals are precipitated or dissolved in much smaller amounts, and do not affect significantly the permeability of the fracture. We can therefore conclude that, according to current numerical simulations, mineral precipitations do not seem to be a direct threat to reservoir performance, even after several years of forced fluid circulation.

Numerous geochemical data collected during the last 20 years as well as multiple production/injection tests allowed to prepare some guidelines for a sound geochemical management of the geothermal fluid during the exploitation of the Soultz reservoir. Variations of main physical and chemical parameters of the fluid during exploitation may hinder a sustainable flow rate at the production well(s) and/or at the injection well(s). Monitoring of selected parameters at a specific frequency is the key for prediction, and understanding, of potential scaling and/or corrosion problems within the geothermal loop and the surface installation. Description of the processes and proposition of a monitoring programme are given in ad hoc tables.

8.2 Recommendations

Section 6 describes in detail the main steps that should be followed to insure a durable exploitation of the Soultz system on a geochemical perspective. An important point is to keep a monitoring program adapted to the evolution of the system. The hydraulic properties of the wells used for production and injection are indirectly monitored by the energy needed for pumping. In addition, the fluid chemical composition should be regularly analysed in order to detect potential modifications in the water-rock interactions in the reservoir, scaling or corrosion in the well casing, etc.

Scaling in the surface installations will hopefully be limited by applying a polymer coating in the locations that are most affected by the barito-celestine precipitates. The extent of corrosion should also be assessed during the periodic maintenance operations.

The high concentration of dissolved solids in the fluid at Soultz bring some challenges to the sampling and analysis procedures in order to obtain concentrations representative of the reservoir brine. One parameter to take into account is the mixing of the reservoir fluid by the important volume of fresh water injected after drilling of the deep wells. This fluid is still present in the produced fluid at an estimated proportion of 2–3 % of the total. Yet the major challenge is to obtain data of a fluid composition that is representative of the fluid in the deep aquifer. Physical and chemical processes affect the fluid properties during the transit of the fluid in the fractured reservoir towards the well and its flow to the wellhead. For instance, silica scaling close to and in the well decreases the silica concentrations in the discharged fluid to about half of the equilibrium concentration with the reservoir rock minerals at the reservoir temperature. Another example is trace elements: analysing concentrations of a few ppb in waters at 100 g l^{-1} of total dissolved solids is a difficult task—mainly because of matrix effects—and no reliable data have been obtained so far.

In order to gain further understanding of the geochemical processes in the Soultz geothermal system, it would be optimal to develop a sampling and analytical procedure that would allow for accurate concentrations, representative of the aquifer fluid. Down-hole sampling is a technique that has been tested in 1999 with mitigated result, but that still leaves room for improvement.

Numerical modelling has long proved an extremely useful tool to understand the processes that do happen or are likely to happen in a geothermal aquifer and on the production installations. In order to complete this study, it would be of high interest to investigate computer simulations of the scaling and corrosion that we observe in the surface installation at Soultz. The precipitation of mineral phases is localized to some very specific locations, which indicates that the process is a consequence of local variations of the temperature and pressure conditions. Numerical models could potentially test alternative designs in the installation that would limit the occurrence of scaling.

A more sophisticated model including all three wells used in the production of the geothermal loop could give insights on the best scheme to use for long-term production. This would have to be carried in close relationship with the teams working on hydraulic properties of the Soultz system.

Finally, it is strongly recommended to continue the geochemical monitoring and develop a robust long-term programme capable of anticipating a negative evolution of the exploitation of the Soultz geothermal reservoir and of the surface installations.

9 References

André, L., and Vuataz, F.-D. (eds.), 2005. Studies and support for the Hot Fractured Rock reservoirs at Soultz-sous-Forêts. State Secretariat for Education and Research Final Report October 2001 – December 2004, OFES Project N° 00.0453, 240 pp.

Andre, L., Spycher, N., Xu, T., Vuataz, F. D., and Pruess, K., 2006. Modeling brine-rock interactions in an enhanced geothermal system deep fractured reservoir at Soultz-sous-Forets (France): a joint approach using two geochemical codes: FRAChem and TOUGHREACT. Lawrence Berkeley National Laboratory report nb. LBNL–62357.

Aquilina, L., Pauwels, H., Genter, A., and Fouillac, C., 1997. Water-rock interaction processes in the Triassic sandstone and the granitic basement of the Rhine Graben: Geochemical investigation of a geothermal reservoir. Geochim. Cosmochim. Acta 61 (20), 4281–4295.

Baticci, F., Genter, A., Huttenloch, P., and Zorn, R., 2010. Corrosion and scaling detection in the Soultz EGS power plant, Upper Rhine Graben, France. Proc. World Geothermal Congress, Bali, Indonesia.

Dezayes, C., Chevremont, P., Tourlière, B., Homeier, G., and Genter, A., 2005. Geological study of the GPK-4 HFR borehole and correlation with the GPK-3 borehole and correlation with the GPK-3 borehole (Soultz-sous-Forêts, France), BRGM/RP-53697-FR report, 2005, 94 pp.

Dezayes, C., Genter, A., and Valley, B., 2010. Structure of the low permeable naturally fractured geothermal reservoir at Soultz. C. R. Geoscience 342, 517–530.

Drummond, J. M., Jr., 1981. Boiling and mixing of hydrothermal fluids: Chemical effects on mineral precipitation, Ph.D. thesis, The Pennsylvania State University, University Park, Pennsylvania.

Genter, A., 2011. Overview of the scientific and technical research program done at Soultz during geothermal exploitation. Soultz Geothermal Conference, 5–6 October 2011, Soultz-sous-Forêts, France, 10.

Genter, A., Cuenot, N., Goerke, X., Bernd, M., Sanjuan, B., and Scheiber, J., 2012. Status of the Soultz geothermal project during exploitation between 2010 and 2012. Proceedings, 37th Workshop on Geothermal Reservoir Engineering, Stanford University, Stanford.

Harvie, C.E., Moller, N., and Weare, J.H., 1984. The Prediction of Mineral Solubilities in Natural Waters: The Na-K-Mg-Ca-H-Cl-SO4-OH-HCO3-CO3-H2O System to High Ionic Strengths at 25°C. Geochimica et Cosmochimica Acta, 48, (4), 723–751. New York, New York: Pergamon Press.

Johnson, J.W., Oelkers, E.H., and Helgeson, H.C., 1992. SUPCRT92: A software package for calculating the standard molal thermodynamic properties of minerals, gases, aqueous species, and reactions from 1 to 5000 bar and 0 to 1000°C. Computers & Geosciences 18(7), 899-947.

Lasaga, A. C., 1984. Chemical kinetics of water-rock interactions. J. Geophys. Res. 89, 4009–4025.

Melchert, B., and Tischner, T., 2011. Hydraulic reservoir monitoring of the Soultz power plant in 2010 and 2011. Soultz Geothermal Conference, 5–6 October 2011, Soultz-sous-Forêts, France, 14.

Mueller, J., Billkova, K., Genter, A., and Seiersten, M., 2010. Laboratory Results of Corrosion Tests for EGS Soultz Geothermal Wells. Proc. World Geothermal Congress, Bali, Indonesia.

Palandri, J.L. and Kharaka, Y.K., 2004. A compilation of rate parameters of water-mineral interaction kinetics for application of geochemical modelling. U.S. Geological Survey Report 2004-1068.

Pauwels, H., Fouillac, C. and Fouillac, A.-M., 1993. Chemistry and isotopes of deep geothermal saline fluids in the Upper Rhine Graben; origin of compounds and water-rock interactions. Geochimica et Cosmochimica Acta, 57 : 2737–2749.

Portier, S. and Vuataz, F.-D. (eds.), 2009. Studies and support for the EGS reservoirs at Soultz-sous-Forêts. State Secretariat for Education and Research Final Report January 2005 – May 2009, OFES/BEW Project N° 03.04.60 — OFEN/BFE Project N° 150'649, 110 pp.

Pruess, K., 1991. TOUGH2: A general numerical simulator for multiphase fluid and heat flow. Lawrence Berkeley Laboratory Report LBL-29400, Berkeley, California, 1991.

Rumpf, B., and Maurer, G.,1993. An experimental and theoretical investigation on the solubility of carbon dioxide in aqueous solutions of strong electrolytes. Berichte der Bunsengesellschaft fuer physikalische chemie, 97(1), 85–97.

Rumpf, B., Nicolaisen, H., Öcal, C., and Maurer, G., 1994. Solubility of carbon dioxide in aqueous solutions of sodium chloride: Experimental results and correlation. Journal of Solution Chemistry, 23(3), 431–448.

Sanjuan, B., Millot, R., Dezayes, C. and Brach, M., 2010. Main characteristics of the deep geothermal brine (5 km) at Soultz-sous-Forêts (France) determined using geochemical and tracer test data. C. R. Geoscience 342, 546–559.

Scheiber, J., Nitschke, F., Seibt, A., and Genter, A., 2012. Geochemical and mineralogical monitoring of the geothermal power plant in Soultz-sous-Forêts (France). Proceedings, 37th Workshop on Geothermal Reservoir Engineering, Stanford University, Stanford, California, Jan. 30 – Feb. 1.

Schellschmidt, R., Schindler, M., Wonik, T., and Ortiz, A., 2010. Temperature profiles in the soultz wells GPK2, GPK3 and GPK4 while and after circulating. Soultz Geothermal Conference, 5–6 October 2011, Soultz-sous-Forêts, France, 13.

Steefel, C.I., and Lasaga, A.C., 1994. A coupled model for transport of multiple chemical species and kinetic precipitation/dissolution reactions with applications to reactive flow in single phase hydrothermal system. Am. J. Sci. 294, 529-592.

Verma, A. and Pruess, K., 1988. Thermohydrological conditions and silica redistribution near high-level nuclear wastes emplaced in saturated geological formations. J. Geophys. Res., 93: 1159–1173.

Vinsome, P. K. W., and Westerveld, J.,1980. A simple method for predicting cap and base rock heat losses in thermal reservoir simulators. J. Canadian Pet. Tech., 19(3), 87–90.

Wolery T., Jove-Colon C., Rard., J., Wijesinghe., A., 2004. Pitzer Database Development: Description of the Pitzer Geochemical Thermodynamic Database data0.ypf. Appendix I in In-Drift Precipitates/Salts Model (P. Mariner) Report ANL-EBS-MD-000045 REV 02. Las Vegas, Nevada: Bechtel SAIC Company.

Xu, T. and Pruess, K., 2001. Modeling multiphase fluid flow and reactive geochemical transport in variably saturated fractured rocks: 1. Methodology. Am. J. Sci., 301, 16–33.

Xu, T., Sonnenthal, E., Spycher, N. and Pruess, K., 2004. TOUGHREACT user's guide: a simulation program for non-isothermal multiphase reactive geochemical transport in variably saturated geologic media. Report LBNL-55460, Lawrence Berkeley National Laboratory, Berkeley, California.

Xu, T., Sonnenthal E., Spycher N., and Pruess, K., (2006). TOUGHREACT - A simulation program for non-isothermal multiphase reactive geochemical transport in variably saturated geologic Media: applications for geothermal injectivity and CO2 geologic sequestration. Computers and Geosciences, 32, 145–165.

Zhang, G., Spycher, N., Xu, T., Sonnenthal, E., and Steefel, C., 2006a. Reactive geochemical transport modeling of concentrated aqueous solutions with TOUGHREACT — Supplement to TOUGHREACT users' guide for the Pitzer ion-interaction model. Report LBNL-57873, Lawrence Berkley National Laboratory, Berkeley, California

Zhang, G., Spycher, N., Sonnenthal, E., and Steefel, C. 2006b, Implementation of a Pitzer activity model into TOUGHREACT for modeling concentrated solutions. Proceedings, TOUGH Symposium 2006, Lawrence Berkeley National Laboratory, Berkeley, California, May 15–17 (Report LBNL-60016).

APPENDICES

Appendix I : FRAChem instructions

To run the 1D model representing a fracture of the Soultz reservoir with *FRAChem* two input files are required: *Input.dat* and *chem_dat*.

Input files

Input.dat

Input.dat is the input file for the *FRACTure* part of *FRAChem* and is generated by *WinFra*, a meshing software created at ETH Zürich. It contains the main information to run *FRAChem*: execution control information, model geometry, element neighbourhood, solver information, time sequences, time steps, coupling information, boundary and initial conditions, load-time functions and sources. Figure 22 shows the beginning of the file Input.dat included with this report. Explanation of the various entries is given below.

Only the most important options useful for a variety of simulations of the Soultz reservoir are given here, in Table 13.

Table 13: Description of the main options of the file Input.dat shown in Figure 22

Option	Control card	Description
`numseq`	`DIMENSION CONTROL CARD`	Number of time sequences, further defined in the TIME SEQUENCE CARDS
`n`	`TIME SEQUENCE CARDS`	Time sequence number
`nstep(n)`	`TIME SEQUENCE CARDS`	Number of time steps in sequence
`ndprt(n)`	`TIME SEQUENCE CARDS`	Output increment for primary variables
`nsprt(n)`	`TIME SEQUENCE CARDS`	Output increment for element variables
`nhplt(n)`	`TIME SEQUENCE CARDS`	Output increment for monitor data
`dt(n)`	`TIME SEQUENCE CARDS`	Time step of actual sequence
	`HYDRAULIC COUPLING SEQUENCES`	The number of lines in this control card must match the number of time sequences
	`TRANSPORT COUPLING SEQUENCES`	The number of lines in this control card must match the number of time sequences
	`COORDINATES`	Lists all the mesh nodes of the model

```
         0
 ein Eingabe File das von WinFra 0.77 erstellt wurde
* EXECUTION CONTROL CARD
*    iexec    iacode    idebug     irank    ireadr    iprtin    iprtut    iprtec
         1         0         0         0         0         0         0         1
* DIMENSION CONTROL CARD
*   numseq    ndhist       nsd     numnp     ngdof    nlvect    nltftn    nptslf
         7         0         3       266         2         2         2         2
* SOLUTION ALGORITHM CONTROL CARD
*     ipcg      isym     ifact     itmax       tol
         1         1        25       400   1.0E-08
* COUPLING CONTROL CARD
*   numegh    numegt    numege     iterh      epsh     itert      epst     itere      epse
         2         2         0         0   1.0E-02         0   1.0E-02         0         0
* TIME SEQUENCE CARDS
*        n     nstep     ndprt     nsprt     nhplt        dt
         1         1         1         1         1   0.0E+00
         2         1         0         1         1   0.0E+01
         3    311040    311040    311040    311040   1.0E+02 ! 1year
         4    311040    311040    311040    311040   1.0E+02 ! 1year
         5    311040    311040    311040    311040   1.0E+02 ! 1year
         6    311040    311040    311040    311040   1.0E+02 ! 1year
         7    311040    311040    311040    311040   1.0E+02 ! 1year
* HYDRAULIC COUPLING SEQUENCES:
*        n     nthyd     niter     alpha      beta     gamma     iterj    relaxj     epsil
         1         0         1       0.0       0.0       0.0         0       0.8   1.0E-06
         2        -1         1       0.0       0.0       0.0         0       0.8   1.0E-06
         3        -1         1       0.0       0.0       0.0         0       0.8   1.0E-06
         4        -1         1       0.0       0.0       0.0         0       0.8   1.0E-06
         5        -1         1       0.0       0.0       0.0         0       0.8   1.0E-06
         6        -1         1       0.0       0.0       0.0         0       0.8   1.0E-06
         7        -1         1       0.0       0.0       0.0         0       0.8   1.0E-06
* TRANSPORT COUPLING SEQUENCES:
*        n   nttrans     niter     alpha      beta     gamma     iterj    relaxj     epsil
         1        -1         1       0.0       0.0       0.0         0       0.8   1.0E-06
         2         0         1       0.0       0.0       0.9         0       0.8   1.0E-06
         3         1         1       0.0       0.0       0.9         0       0.8   1.0E-06
         4         1         1       0.0       0.0       0.9         0       0.8   1.0E-06
         5         1         1       0.0       0.0       0.9         0       0.8   1.0E-06
         6         1         1       0.0       0.0       0.9         0       0.8   1.0E-06
         7         1         1       0.0       0.0       0.9         0       0.8   1.0E-06
* MONITOR NODES
*      Knr       dof      Spez
******** WINFRA DOESN'T CREATE MONITOR NODES YET ! ************
* COORDINATES
*      n         gen  x(1,n)    x(2,n)    x(3,n)
         1         0     57.50      0.05      0.00
         2         0     57.50      0.00      0.00
         3         0     65.50      0.00      0.00
         4         0     65.50      0.05      0.00
         5         0     53.50      0.00      0.00
         …
         (continues for all grid blocks)
```

Figure 22: First lines of file Input.dat

```
* IDENTIFICATION OF BOUNDARY CONDITIONS
*       n         ne       ng       id1       id2    ...
c      36        36        1         1         0
c       7         7        1         1         1
        8         8        1         1         1
       35        35        1         1         0
       55        55        1         0         1
       56        56        1         0         1
       57        57        1         0         1
…
            (continues for all grid blocks with defined boundary conditions)
```

Figure 23: Input.dat fragment showing the indentification of boundary conditions

Table 14: Variables of Input.dat file given in Figure 23

Option	Control card	Description
`n`	`INDENTIFICATION OF BOUNDARY CONDITIONS`	First node number
`ne`	`INDENTIFICATION OF BOUNDARY CONDITIONS`	Last node number
`ng`	`INDENTIFICATION OF BOUNDARY CONDITIONS`	Nodal increment
`id(1,n)`	`INDENTIFICATION OF BOUNDARY CONDITIONS`	Identification of BC for 1st DOF. 0: Neumann BC (no declaration necessary) 1: Dirichlet BC (primary variable) 2: ? time derivative of primary variable 3: ? acceleration (only elasticity)

```
* VALUES OF BOUNDARY CONDITIONS
*       n        gen      f(1,n)    f(2,n)      ...
        55         0         0       200
        56         0         0       200
        57         0         0       200
        58         0         0       200
        61         0         0       200
        62         0         0       200
        64         0         0       200
        67         0         0       200
        68         0         0       200
        70         0         0       200
…
(some sections skipped)


* HYDRO - THERM. material properties
*     Mat    h-Cond1   h-Cond2   h-Cond3  St.coef.    Poros.     area FactApert0
*           xy-pitch   xz-roll    yz-yaw mol.Konz.
*     Mat    t-Cond1   t-Cond2   t-Cond3    rhocpf    rhocpm   Disp.x1   Disp.x2      area
*           xy-pitch   xz-roll    yz-yaw   Absorpt
* matrix
         1   1.0E-15   1.0E-15   1.0E-15         0         0       0.5         1
                   0         0         0         0
         1         3         3         3   4200000   2650000         0         0       0.5
                   0         0         0         0
* matrix
         2   1.0E-15   1.0E-15   1.0E-15         0         0       0.5         1
                   0         0         0         0
         2         3         3         3   4200000   2650000         0         0       0.5
                   0         0         0         0
* Z-COMPONENT
         0         1         0
* ELEMENT CARDS
*    El-nr       Mat       ien  ...
         1         1         1         2         3         4         0
         2         1         5         2         1         6         0
         3         1         7         8         9        10         0
         4         1         9        11        12        10         0
         5         1        12        11         5         6         0
         6         1        13        14        15        16         0
         7         1         3        14        13         4         0
         8         1        17        18        19        20         0
         9         1        21        22        23        24         0
…
(continues)
```

Figure 24: Fragment of Input.dat file

Table 15: Variables of Input.dat file given in Figure 24

Option	Control card	Description
`n`	`VALUES OF BOUNDARY CONDITIONS`	Node number
`f(1,n)`	`VALUES OF BOUNDARY CONDITIONS`	Value of BC for 1st DOF
`f(2,n)`	`VALUES OF BOUNDARY CONDITIONS`	Value of BC for 2nd DOF
`Mat`	`HYDRO - THERM. material properties`	Material identification
`h-Cond1 to h-Cond3`	`HYDRO - THERM. material properties`	Hydraulic conductivity in three dimensions. Three same values if isotropic material
`St.Coef`	`HYDRO - THERM. material properties`	Specific storage coefficient
`poros(m)`	`HYDRO - THERM. material properties`	Porosity
`area(m)`	`HYDRO - THERM. material properties`	Area / thickness
`rhocpm`	`HYDRO - THERM. material properties`	Material specific weight (g m^{-3})
`ELEMENT CARDS`	`HYDRO - THERM. material properties`	Lists all nodes of this material

chem.dat

chem.dat is the input file for the *CHEMTOUGH* part of *FRAChem*. It contains all geochemical information. Since *chem.dat* is described in detail in Durst (2002), only a brief overview is given here. The three entries in the first line are the maximum relative concentration variations allowed for a chemical species, the number of chemical outputs and the coupling parameter. If the coupling parameter is true (.T.), the porosity and permeability variation calculated in the chemical module is passed to *FRACTure*. In contrast, if the coupling parameter is false (.F.), *FRACTure* will not take into account these variations. In the second line the number of reactions, of species and of gas reactions are listed. However, gas reactions are not yet included in *FRAChem*. The following block (from H_2O to CO_3^{2-}) contains the electrical charge, phase of species (L for liquid and S for solid), concentration in mol/kg, molecular weight in g/mol, volume mass of solid in kg/m^3 and the coefficients for the calculation of the activity coefficients for each species in the system. In the next block, the information on the reactions is listed. The name of the reaction is indicated followed by the stoichiometric coefficients of the basis species in the reaction and the type of reaction on the next line. ‘1’ indicates aqueous species, ‘4’ solid species at equilibrium and ‘5’ kinetic reactions. The following line lists the coefficients for the calculation of logK. On the last line, five rate data parameters for non-equilibrium reactions are listed: the reaction surface area (is calculated by *FRAChem*), the proportion of mineral in grain type porous space, the ratio between grain permeability and fracture permeability, and the mineral number. The last block contains the information on the injection, production and surface installation volume. The first line after INJ and PROD indicates the number of injection and production wells, respectively. The following lines list the element number of the wells and the injection or production rates in m^3/s. By setting a negative index for the injection rate, the rates are determined from the *FRACTure* fluid velocities. After SURF the volume of the surface element, temperature and pressure are set.

FORMAT OF FRAChem OUTPUT FILES

output.dat

Contains a summary of the model set up as well as debugging information. Whenever a simulation fails to run, an error message is printed into *output.dat*. At the end of a successful simulation the computation time is printed.

disX.dat

disX.dat contains for each node the co-ordinates, temperature and pressure at specified time steps. The first number in the TITLE indicates the number of the file and the second the time in seconds. The temperature is given in °C and the pressure in Pa. The second block lists the element-node connections so that the file format is readable by the visualisation software *Tecplot*.

advX.dat and hflX.dat

The *advX.dat* and *hflX.dat* files contain the x-, y- and z-component of the velocity and the x-, y- and z-component of the heat flow at each element mid point, respectively. Again, the first number in the TITLE indicates the number of the file and the second number the time in seconds. The velocity is given in m/s and the heat flow in W/m^2. Also these files are readable by *Tecplot*.

chem_output.dat

The *chem_output.dat* lists the chemical results at specified time steps. The first line lists the time in seconds, the time in days, the number of chemical and transport iterations. Further, for all active elements and the surface element (element 0) the temperature in °C, pressure in Pa, porosity, permeability in m^2, pH, ion concentrations in mol/kg and the reaction rates for minerals in mol/m^3/s are printed.

mon_node_elX.dat

To monitor the temporal evolution of the parameters for all active elements a *mon_node_elX.dat* is printed. The files contain the time in seconds, pressure in Pa, porosity, permeability in m^2, pH, ion concentrations in mol/kg, mineral concentrations in mol/kg, and the mineral reaction rates in mol/m^3/s. The file format is readable by *Tecplot*.

Model set-up

The main application of the code FRAChem was the modelling of a simple case, which reproduces at a real scale what can happen if a cooled Soultz fluid is reinjected in a hot reservoir. Injection and production wells are linked by fractured zones and surrounded by the granite matrix. The model is composed of 1250 fractured zones. Each fractured zone has an aperture of 0.1 m, a depth of 10 m, a porosity of 10 %, and contains 200 fractures. Initially the temperature was set to the reservoir temperature of 200 °C. One of these fractured zones is modelled with the assumption that the fluid exchange with the surrounding low permeability matrix is insignificant.

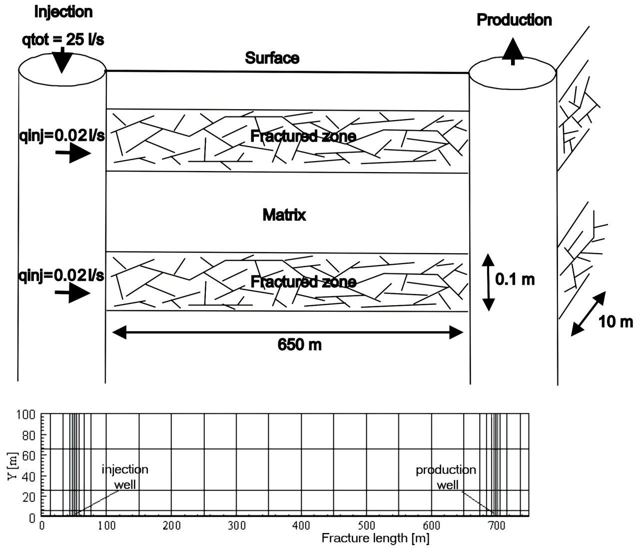

Figure 25: Simplified physical model and spatial discretization of the Soultz reservoir.

The model schematised on Figure 25 consists of a single 650 m long, 0.1 m wide and 10 m deep fractured zone composed of 25 1D elements, surrounded by rock matrix. Due to the symmetrical shape of the model, only the upper part of the fractured zone is considered in the simulation. The area is discretized into 222 2D elements (Figure 1).

The size of the elements ranges from a minimum of 0.5 m x 0.05 m near the injection and the production wells to a maximum of 50 m x 35 m. Considering a production rate of 25 $l.s^{-1}$, the fluid was re-injected in each of the fractured zones at a rate of 2×10^{-2} $l\ s^{-1}$ at a constant temperature of 65 °C. During this simulation a constant overpressure of 8 MPa was assumed at the injection well and a hydrostatic pressure at the production well. Dirichlet boundary conditions were applied to the upper, left and right side of the model.

Appendix II : Selected gas analyses

Table 16: Selected gas concentrations and Gas to Liquid Ratios (GLR) of samples collected from production well GPK2.

Sampling year	GLR % vol.	GLR % mass	CO_2 % vol.	N_2 % vol.	He % vol.	H_2 % vol.	CH_4 % vol.
1999	29		62	27	0.65	6.0	5.0
2005			57	34	2	1.9	6.3
2010	75.00	0.13	85.2	9.94	0.84	0.82	2.24
2010	107.00	0.19	86.5	10.1	0.80	1.12	2.29
2011	104.00	0.18	83.5	11.6	0.76	0.4	2.46

Appendix III : List of publications by the Centre for Hydrogeology and Geothermics (CHYN) on the Soultz-sous-Forêts project

Journals

André L., Rabemanana V. and Vuataz F.-D., 2006. Geochemical modelling of water-rock interactions and implications on the properties of the Soultz fractured reservoir. Geothermics, 35, 507-531.

Portier S., Vuataz F.-D., Nami P., Sanjuan B. and Gérard A., 2009. Chemical stimulation techniques for geothermal wells: experiments on the three-well EGS system at Soultz-sous-Forêts, France. Geothermics, 38, 349-359.

Portier S. and Vuataz F.-D., 2010. Developing the ability to model acid-rock interactions and mineral dissolution during the RMA stimulation test performed at the Soultz-sous-Forêts EGS site, France. Comptes Rendus Geoscience, 342, 668-675.

Rabemanana V., Durst P., Bächler D., Vuataz F.-D. and Kohl Th., 2003. Geochemical modelling of the Soultz-sous-Forêts Hot Fractured Rock system: comparison of two reservoirs at 3.8 and 5 km depth. Geothermics, 32(4-6), pp. 645-653.

Proceedings

André L., Rabemanana V. and Vuataz F.-D., 2005. Geochemical modelling of water-rock interactions and implications on the properties of the Soultz fractured reservoir. Proc. EHDRA Scientific Conference, March 17-18, 2005, Soultz-sous-Forêts, France.

André L. and Vuataz F.-D., 2005. Simulated evolution of reservoir properties for the Enhanced Geothermal System at Soultz-sous-Forêts: the role of hot brine-rock interactions. Proceedings, 30th Workshop on Geothermal Reservoir Engineering. Stanford University, Stanford, California, January 31 - February 2, 2005.

André L., Spycher N., Xu T., Pruess K. and Vuataz F.-D., 2006. Comparing FRAChem and TOUGHREACT for reactive transport modeling of brine-rock interactions in Enhanced Geothermal Systems (EGS). Proc. 31st Workshop on Geothermal Reservoir Engineering, Jan. 30-Febr. 1, 2006, Stanford University, Stanford, California.

Durst P. and Vuataz F-D, 2000. Fluid-rock interaction in hot dry rock reservoirs. A review of the HDR sites and detailed investigations of the Soultz-sous-Forêts system. World Geothermal Congress 2000 (WGC 2000), May 28 – June 10, 2000, Kyushu-Tohoku, Japan.

Durst P. and Vuataz F-D, 2001. Geochemical modelling of the Soultz-sous-Forêts Hot Dry Rock system, brine rock interactions in a deep hot fracture granite reservoir, Proceedings 26th Workshop on Geothermal Reservoir Engineering, January 29-31, 2001, Stanford University, Stanford, California, SGP-TR-168.

Portier S., André L., Vuataz F.-D., 2006. Modelling geochemical effects of acid treatments and comparison with field observations at Soultz-sous-Forets geothermal site. Proc. ENGINE Scientific Workshop 3, « Stimulation of reservoir and microseismicity », Kartause Ittingen, Zürich, Switzerland, June 29-July 1, 2006.

Portier S., André L. and Vuataz F.-D., 2006. Review of chemical stimulation techniques and results of acid injection experiments at Soultz-sous-Forets. Proc. EHDRA Scientific Conference, Soultz-sous-Forêts, France, June 15-16, 2006.

Portier S., André L. and Vuataz F.-D., 2007. Evolution of an EGS reservoir simulated by modelling the geochemical effects of forced fluid circulation at Soultz-sous-Forêts. Proc. EHDRA Scientific Conference, Soultz-sous-Forêts, France, June 28-29, 2007.

Portier S., André L., Vuataz F.-D. and Kohl T., 2007. Modelling the impact of forced fluid-rock interactions on reservoir properties at Soultz-sous-Forêts EGS geothermal site. Proc. European Geothermal Congress 2007, Unterhaching, Germany, 30 May - 1 June 2007.

Portier S., Kühn M. and Vuataz F.-D., 2007. Comparing FRAChem and SHEMAT for the modelling of brine-rock interactions in Enhanced Geothermal Systems. Proc. European Geothermal Congress 2007, Unterhaching, Germany. 30 May - 1 June 2007.

Portier S., André L. and Vuataz F.-D., 2008. Reactive transport modelling of forced fluid circulation and scaling tendencies in fractured granite at Soultz-sous-Forêts EGS geothermal site. Proc. EHDRA Scientific Conference, Soultz-sous-Forêts, France, September 24-25, 2008.

Portier S., André L. and Vuataz F.-D., 2008. Review on chemical stimulation techniques in oil industry and applications to geothermal systems. Technical Report ENGINE, WP4, ENhanced Geothermal Innovative Network for Europe, 39 pp.

Portier S., and Vuataz F.-D., 2010. Modelling Acid-Rock Interactions and Mineral Dissolution During RMA Stimulation Test Performed at the Soultz-sous-Forêts EGS Site, France. Proc. World Geothermal Congress 2010, 25-29 April 2010, Bali, Indonesia.

Rabemanana V. and Vuataz F.-D., 2003. Coupled modelling of hot brine-rock interaction at Soultz-sous-Forêts enhanced geothermal system. Proceedings Conference on structures in the continental crust and geothermal resources (Abstract only), September 2003, Siena, Italy.

Rabemanana V., André L. and Vuataz F.-D., 2004. Simulations of hot brine-rock interactions and consequences on reservoir properties - Enhanced Geothermal System at Soultz-sous-Forets, France. Réunion des Sciences de la Terre, September 20-26, 2004, Strasbourg, France

Rabemanana V., Vuataz F.-D., Kohl Th. and André L., 2005. Simulation of mineral precipitation and dissolution in the 5-km deep enhanced geothermal reservoir at Soultz-sous-Forêts, France. Proceedings World Geothermal Congress WGC2005, 24-29 April 2005, Antalya, Turkey.

Reports

André L., Spycher N., Xu T., Pruess K. and Vuataz F.-D., 2006. Modelling brine-rock interactions in an Enhanced Geothermal System deep fractured reservoir at Soultz-sous-Forêts (France): a joint approach from two geochemical codes: FRAChem and TOUGHREACT. Lawrence Berkeley National Laboratory, Berkeley. LBNL Collaboration Report, LBNL-62357, 71 pp.

André L. and Vuataz F.-D. (eds.), 2005. Studies and support for the Hot Fractured Rock reservoirs at Soultz-sous-Forêts. With the contributions of D. Bächler, P. Durst, K. Evans, R. Hopkirk, T. Kohl, T. Mégel, V. Rabemanana & F.-D. Vuataz. 5th FP of the European Commission, EC Contract N° ENK5-CT2000-00301. Federal Office for Education and Science Project – OFES, N° 00.0453, final report.

Bächler D., Durst P., Evans K., Hopkirk R., Kohl Th., Megel Th., Rabemanana V. and Vuataz F.-D., 2005. Studies and support for the Hot Fractured Rock reservoirs at Soultz-sous-Forêts. Federal Office for Education and Science Project – OFES – N° 00.0453.

Durst P. and Vuataz F-D, 2001. Fluid-rock interactions and geochemical modelling of the formation brine in the fissured reservoir of Soultz-sous-Forêts Hot Dry Rock test site. Federal Office for Education and Science, final report, project 98.0008-3, CHYN, Neuchâtel, Switzerland, 149 p.

Durst P., 2002. Geochemical modeling of the Soultz-sous-Forêts Hot Dry Rock test site: coupling fluid-rock interactions to heat and fluid transport. Thèse soutenue à la faculté de Sciences de l’Université de Neuchâtel (Suisse) le 23 mai 2002.